

Original Article

Boosting immune surveillance by low-dose PI3K inhibitor facilitates early intervention of breast cancer

Jinyang Wang^{1#*}, Yuan Zhang^{1*}, Yi Xiao^{1*}, Xiangliang Yuan¹, Ping Li¹, Xiao Wang¹, Yimin Duan¹, Victoria L Seewaldt^{2,3}, Dihua Yu^{1,4}

¹Department of Molecular and Cellular Oncology, The University of Texas MD Anderson Cancer Center, Houston, Texas, USA; ²Department of Population Sciences, City of Hope, Duarte, California, USA; ³Comprehensive Cancer Center, City of Hope, Duarte, California, USA; ⁴Cancer Biology Program, The University of Texas MD Anderson Cancer Center UT Health Graduate School of Biomedical Sciences, Houston, Texas, USA; #Current address: Department of Pathology, Guangdong Provincial People's Hospital, Guangdong Academy of Medical Sciences, Guangzhou, Guangdong, China. *Equal contributors.

Received November 8, 2020; Accepted December 7, 2020; Epub May 15, 2021; Published May 30, 2021

Abstract: Prevention of estrogen receptor-negative (ER-) breast cancer is an unmet challenge, although tamoxifen and aromatase inhibitors can successfully decrease the incidence of ER-positive (ER+) breast cancer. PI3K pathway activation has been detected in tamoxifen-resistant ER- breast lesions of patients. Here, we further ratified that the PI3K pathway is significantly activated in premalignant ER- breast lesions compared with paired normal tissues of patients, which prompted our assessment of targeting PI3K on inhibition of ER- mammary tumor initiation and progression. Both genetic knockdown of PIK3CA or intervention with low-doses of a PI3K inhibitor (GDC-0941) prevented the dysplasia phenotype of semi-transformed human ER- mammary epithelial cells in 3-dimensional culture *in vitro*. Importantly, low-dose GDC-0941 treatment significantly delayed mammary tumor initiation in the MMTV-*neu* mouse model without exhibiting discernable adverse effects. Interestingly, increased CD8⁺/GZMB⁺ T-cells were detected in mammary tissue after GDC-0941 treatment, suggesting enhanced immune surveillance. Mechanistically, elevated expression of potent T-cell chemo-attractants, including CCL5 and CXCL10, were detected both *in vitro* and *in vivo* after GDC-0941 treatment. Furthermore, inhibition of PI3K significantly increased T-cell recruitment in a CCL5/CXCL10-dependent manner. In human ER- breast cancer, PI3K activation is correlated with significantly reduced CCL5, CXCL10 and CD8A expression, suggesting that the decreased CD8⁺ T-cell recruitment and escape of immune surveillance may contribute to ER- breast cancer development. In summary, our study indicates that low-dose PI3K inhibitor treatment may intervene early stage ER- breast cancer development by enhancing immune surveillance via CCL5/CXCL10.

Keywords: PI3K/Akt, ER- breast cancer, prevention, immune surveillance

Introduction

Elucidating the molecular mechanisms involved in early stage breast cancer development can facilitate early detection and prevention, which are critical for reducing the morbidity and mortality of breast cancer. Large-scale clinical trials on breast cancer prevention showed that selective estrogen receptor modulators (e.g., tamoxifen) and aromatase inhibitors could reduce incidence of estrogen receptor-positive (ER+) breast tumor in high-risk populations by approximately 50% in various age groups [1, 2]. However, no effective agents are available for pre-

vention of estrogen receptor negative (ER-) breast cancer [3-5], which has poorer clinical outcomes compared with ER+ breast cancer. Therefore, there is an urgent need to develop prevention and early intervention strategies for ER- breast cancer.

The phosphatidylinositol-3-kinase (PI3K)/Akt intracellular signaling pathway is involved in various cellular functions, e.g., proliferation, apoptosis, and metabolism, which play critical roles in cancer [6]. In many cancers, this pathway is overactive, leading to reduced apoptosis and accelerated proliferation [7]. Furthermore,

PI3K inhibitor enhances immune surveillance in breast cancer

several studies have shown that the PI3K/Akt pathway is frequently upregulated in breast cancer [8-10]. PI3K/Akt activation is strongly associated with poor prognosis in patients with HER2+/ER- breast cancer [11-13]. In our previous study, profiling of key signaling proteins and pathways by reverse phase protein array uncovered high levels of PI3K/Akt activation in breast tissue samples from women with atypical hyperplasia (ADH) and ductal carcinoma in situ (DCIS) compared with normal tissue, and we detected the PI3K/Akt signaling pathway activation in the early stage of breast disease [14]. These findings suggest that PI3K/Akt activation in mammary atypia could drive initiation and progression of ER- breast cancer. Several PI3K inhibitors-including GDC-0941-have been clinically tested for cancer treatment with tolerable toxicity [15]. We postulate that low doses of PI3K/Akt-targeting agents may be applicable for safe and effective prevention of ER- breast cancer.

Cancer immune surveillance refers to the ability of immune cells to recognize and eliminate premalignant and malignant cells before they can cause harm, thus immune surveillance is critical in cancer prevention. Trafficking of immune cells in tumors is mediated by chemokines, which are also altered during tumor initiation and progression [16]. C-X-C motif chemokines, including CXCL9, CXCL10, and CXCL11, as well as CC chemokines such as CCL3, CCL4, and CCL5, show tight correlations with T-cell infiltration in the tumor microenvironment (TME) and are associated with better clinical outcomes in some cancer types [17]. Some studies have shown a relationship between PI3K/Akt pathway activation in cancer cells and suppression of T-cells in the TME [18, 19]. Therefore, we envisage that targeting the PI3K/Akt pathway using low-dose PI3K inhibitor might also influence T-cell mediated immune surveillance that prevent early stage ER- breast cancer development. The purpose of this study was to determine the effect of low doses of a PI3K inhibitor on chemoprevention of ER-breast cancer.

Materials and methods

Cell lines and cell culture

MCF10A cell line was purchased from American Type Culture Collection (ATCC) and cultured in

DMEM/F12 (Caisson No. DFL13) supplied with 5% horse serum (Thermo Fisher Scientific, 16050122), 20 ng/mL EGF, 100 ng/mL cholera toxin, 0.5 µg/mL hydrocortisone, 10 µg/mL insulin, 50 units/mL penicillin, and 50 µg/mL streptomycin as previously described [2]. McNeuA and N202 cell lines were established from a mammary tumor originating from a female MMTV-*neu* transgenic mouse and cultured in DMEM with 4.5 g/L glucose (Corning No. 10-013-CV) supplied with 10% FBS (Thermo Fisher Scientific, SH3007103) [20]. HCC-1569 cell line was purchased from ATCC and cultured in RPMI-1640 (Caisson No. RPL09) supplied with 10% FBS. All cell lines had been tested for mycoplasma contamination.

RNA interference and stable cell line generation

The shRNAs for PIK3CA (V3LHS-364628, V3LHS-364671) were obtained from MD Anderson Cancer Center's shRNA core facility. The sequence for clone V3LHS-364628 and V3LHS-364671 were 5'-TCTTGAGTAACACTTACGA-3' and 5'-TTACCACACTGCTGAACCA-3', respectively. The shRNA gene knockdown lentiviral vectors and its packaging plasmid (psPAX2) as well as envelope plasmid (pMD2G) were transfected into 293T cells together using the LipoD293 reagent (SignaGen, No. SL100668) according to the manufacturer's instructions. After 48 h, the lentivirus-containing media was collected, filtered with a 0.45-µm filter, and used to infect MCF10A cells in the presence of 10 µg/mL polybrene for 24 h. The infected cells were selected by 2 µg/mL puromycin (InvivoGen, 58-58-2) for 5 days based on the drug selection genes of the introduced vectors.

Cell proliferation assay

Cells were seeded at 1000 cells/well in sextuplicate in 96-well cell culture plates. 20 µL of 5 mg/mL MTT (3-(4,5-dimethylthiazol-2-yl)-2,5-diphenyltetrazolium bromide) (Thermo Fisher Scientific, M6496) in PBS were added into each well and incubated for 2 h at 37°C in the dark. After 2 h of incubation, medium with MTT was removed and replaced with 100 µL of DMSO and vibrated for 5 min on a shaking table to solubilize the intracellular purple formazan, which was analyzed at the absorbance of 570 nm and 620 nm with a microtiter plate reader (BioTek).

PI3K inhibitor enhances immune surveillance in breast cancer

Cell apoptosis assay

Cell apoptosis was detected using FITC Annexin V apoptosis detection kit (BD Biosciences, No. 556547). Briefly, cells were treated with vehicle or GDC-0941 (0.3 μ M or 3 μ M) overnight, washed with cold PBS and resuspended in 1X Binding buffer. 5 μ L of FITC Annexin V and 5 μ L of propidium iodide (PI) were added in each sample, incubated for 15 min at room temperature in the dark, and then analyzed by Flow Cytometry. Early (Annexin V⁺, PI⁻) and late apoptotic cells (Annexin V⁺, PI⁺) were counted as total cells that underwent apoptosis.

Western blotting analysis

Western blotting was performed as previously described [21]. The following Primary antibodies were used: ErbB2 (Cell Signaling, No. 4290), p110 α (Cell Signaling, No. 4255), phospho-Akt (Cell Signaling, No. 4060S), (pan) Akt (Cell Signaling, No. 4691), β -actin (Sigma, No. AC-15). The signal was detected by ECL (Amersham) following the manufacturer's instructions. Images shown in figures are representative of 3 independent experiments.

Three-dimensional cell culture assay

Three dimensional (3D) culture assay was performed following the protocol as previously described [22]. Cells were seeded at 1000 cells/well in culture slides (BD Falcon, No. 354108) and cultured in medium containing 2% Matrigel (BD Biosciences), and the medium was replaced every 3 days. At day 4, the 10A. B2 cells were treated with either vehicle or GDC-0941 (LC Laboratories) for another 5 days. Phase-contrast images were captured at day 9 and day 14. At day 9, acini were stained with anti-cleaved caspase-3 (Cell Signaling, No. D175), laminin 5 (Millipore, No. MAB1947), and DAPI (Abcam, No. ab104139). At day 14, acini were stained with anti-Ki-67, laminin 5, and DAPI. The images were taken at 60 \times magnification using a Zeiss confocal microscope. ImageJ software was used to measure acinar size.

Immunofluorescence staining of cells

Immunofluorescence staining on cells in 3D culture was performed as previously described [14]. 3D cultures were fixed with 4% PFA, permeabilized with 0.3% Triton X-100, washed 3

times with PBS/glycine buffer, and blocked with IF buffer (10% goat serum, 0.2% Triton X-100, and 0.05% Tween 20) for 1 h. Antibodies were diluted in IF buffer and incubated overnight at 4 $^{\circ}$ C followed by incubation with Goat Anti-Rabbit 488 and Alexa Fluor Goat Anti-Mouse 594 (Invitrogen, No. 0-11038, A-11005, 1:300 dilution) at 37 $^{\circ}$ C for 1 h. Samples were covered with anti-fade mounting medium with DAPI (Abcam) and analyzed with a Zeiss LSM 880 laser scanning confocal microscope.

Animal experiments

All animal experiments were carried out in accordance with protocols approved by the Institutional Animal Care and Use Committee of The University of Texas MD Anderson Cancer Center. Female MMTV-*neu* mice at 10 weeks of age were treated with GDC-0941 at 50 mg/kg (n=29) or vehicle (n=29, 0.5% hydroxypropyl methylcellulose with 0.1% Tween 80) by oral gavage once daily until tumors were palpable. The median tumor-free survival time was referred as T (50). 8-, 10- and 15-weeks after treatment, 4-5 mice were euthanized in each group and the fourth pair of normal-looking mammary fat pads (MFPs), bones, and bone marrow were isolated. All sample tissues were collected for histological analyses, flow cytometry, and RT-PCR. FVB mice were treated with oral gavage of vehicle (n=3) or GDC-0941 at 20 mg/kg (n=3) and 100 mg/kg (n=4) for two weeks, and then examined toxicity of GDC-0941.

RNA extraction and RT-PCR

Total RNA of MFP cells was extracted using Trizol LS (Molecular Research Center, No. TS120) according to the manufacturer's protocol. Total RNA was isolated using Trizol reagent (Molecular Research Center, No. TR118) from the tissue samples. RNA was reverse transcribed into cDNA using iScript cDNA Synthesis Kit (Bio-Rad, No. 1708891). Real-time PCR was performed in 96-well plates on a CFX96 Touch Real-Time PCR Detection System (Bio-Rad) using iTaq Universal SYBR Green Supermix (Bio-Rad, No. 1725121). Targeted mRNA expression in each sample was normalized to endogenous control (18S). The relative mRNA expression was quantified by 2 $^{-\Delta\Delta C_t}$ method. Each experiment was repeated at least 3 times. The following primers were used to detect cor-

PI3K inhibitor enhances immune surveillance in breast cancer

responding mRNAs in the RT-PCR analyses: CCL5 FQP, 5'-TTTGCCTACCTCTCCCTCG-3'; CCL5 RQP, 5'-CGACTGCAAGATTGGAGCACT-3'; CXCL10 FQP, 5'-CCAAGTGTGCCGTCATTTTC-3'; CXCL10 RQP, 5'-GGCTCGCAGGGATGATTTCAA-3'; 18S FQP, 5'-GTAACCCGTTGAACCCATT-3'; and 18S RQP, 5'-CCATCCAATCGGTAGTAGCG-3'.

Immunohistochemistry and immunofluorescent staining of tissue

Immunohistochemical staining was conducted as previously described [23]. The slides were incubated at 4°C overnight with the following primary antibodies: phospho-Akt (Cell Signaling, No. 4060S, 1:200), Ki-67 (Abcam, No. ab15580, 1:1000), CD45 (BioLegend, No. 103102, 1:100), CD3 (Abcam, No. ab16669, 1:100), CD8 (Abcam, No. ab217344, 1:100), and GZMB (Abcam, No. ab4059, 1:100). Positive control and negative control slides were included in each staining. The stained MFP samples were scored using the immunoreactive score according to multiplication of staining intensity scores and percentage of positive cell scores. Immunohistochemical staining and quantification were performed in a double-blind manner. For immunofluorescent staining, slides were incubated with Alexa Fluor secondary antibodies (Invitrogen) and analyzed by Zeiss LSM 880 laser scanning confocal microscope.

Human lymphocyte generation

Human leukocyte concentrate (buffy coat) was collected from healthy blood donor volunteers by MD Anderson Blood Donor Center. Written informed consent was obtained from all participating blood donors and the use of anonymized leftover specimens for scientific purposes was approved by the Ethics Committee of the MD Anderson Cancer Center. For the generation of lymphocytes, peripheral blood of healthy individuals was applied to a Ficoll gradient (BD), lymphocytes were collected and cultured in RPMI-1640 culture medium (10% FBS, 2 mM glutamine, 1% sodium pyruvate, 1% HEPES, 1% MEM non-essential amino acids, 50 µM 2-mercaptoethanol).

T-cell recruitment assay

T-cell recruitment assays were performed as previously described [24] with minor modifications. Briefly, splenocytes of FVB mice were col-

lected and were activated with CD3/CD28 (BioLegend, No. 100238, 102102) for 24 h. N202 cells pretreated with either vehicle or 0.3 µM GDC-0941 for 48 h were seeded onto 24-well plates, and activated splenocytes were then added on 3-µm hanging cell culture inserts (Millicell, No. MCMP24H48) placed in a 24-well plate. After overnight incubation, splenocytes that migrated to the 24 wells were collected, counted, and stained with fixable viability dye (Invitrogen, No. 65-0863-14) followed by APC/Cyanine7 anti-mouse CD45, FITC anti-CD3, PerCP/Cyanine5.5 anti-CD8, PE anti-CD4, and APC anti-IFN-γ (BioLegend, No. 103116, 100204, 100734, 100408, 505810) antibodies and analyzed by FACS Canto II flow cytometer. For chemokine blockade, anti-CCL5, anti-CXCL10 antibodies and IgG control (R&D systems, No. AF478, AF466, AF007) were added after GDC-0941 treatment in N202 cells, and T-cell recruitment assay was performed as stated above.

Terminal deoxynucleotidyl transferase dUTP nick end labeling staining

Paraffin-embedded tissue slices were dewaxed, rehydrated, fixed, washed with PBS and permeabilized with 20 µg/ml Proteinase K solution at room temperature. After washing with PBS, the slides were dipped in a terminal deoxynucleotidyl transferase dUTP nick end labeling (TUNEL) reaction mixture (Promega, No. G7360) for 60 min at 37°C in a humidified chamber. The reaction was stopped with SSC, washed with PBS, and blocked with 0.3% hydrogen peroxide for 3 min. Subsequently, the slides were incubated with 100 µl streptavidin HRP for 30 min at room temperature. The slides were stained with DAB and visualized with a light microscope.

Bioinformatics analysis

A 32-gene transitional signature of the PI3K/Akt/mTOR pathway was adapted from previous publication [25]. Gene expression data of CCL5, CXCL10, CD8A, and the 32-genes were obtained from different sources accordingly. Gene expression data of matched breast tissues, DCIS, and IDC is available from GSE14548 (<https://www.ncbi.nlm.nih.gov/geo/query>). The data of atypical ductal breast hyperplasia, DCIS, and IDC can be download from supporting information from the publication [26]. The TCGA ER- breast cancer gene expression data

(175 cases) is downloaded from TCGA data portal (<https://tcga-data.nci.nih.gov/tcga/dataAccessMatrix.htm>). Another ER- breast cancer gene expression data from 123 patients is obtained from GSE20685 [27]. The correlations between *CCL5* vs *CD8A* and *CXCL10* vs *CD8A* were measured using Pearson correlation coefficient *r*. The 32-gene signature of PI3K pathway was calculated using Z-score of the 32 genes. The ER- patients were divided to PI3K-score high (top one third of the highest PI3K signature score) and PI3K-score low (bottom one third of the lowest PI3K signature score) based on the 32-gene signature.

Statistical analysis

Statistics were analyzed either by 1-way ANOVA or Student *t* test where applicable. Tumor-free survival analyses were performed using the Kaplan-Meier method and Wilcoxon test. Statistical analysis was performed using SPSS (16.0; SPSS, Inc.) and GraphPad Prism (Prism 8.0; GraphPad Software Inc.) packages. Error bars represent means \pm SD. A *P* value < 0.05 was considered significant. All quantitative experiments were repeated in at least 3 independent tests.

Results

Blocking PIK3CA prevents the dysplasia phenotype of 10A.B2 mammary epithelial cells

Aberrant PI3K/Akt activation has been found in more than 27% of breast cancers [28], including HER2+ breast cancer. Bioinformatic analysis of early stage breast cancer reveals a significantly increased PI3K activation in ductal carcinoma *in situ* (DCIS) compared with patient-matched normal breast tissue (**Figures 1A, S1**) [14]. Atypical hyperplasia lesions showed similarly increased PI3K activation as found in DCIS and invasive ductal carcinoma (IDC) stage (**Figure 1B**), indicating PI3K activation is a very early event in breast cancer initiation. To determine whether PI3K pathway activation contributes to breast cancer initiation, we knocked down PIK3CA using shRNA (shPIK3CA) in the semi-transformed 10A.B2 cell line, a subline of MCF10A human mammary epithelial cells (MEC) that stably overexpress exogenous ErbB2 gene and recapitulate the dysplasia phenotypes of DCIS in three dimensional (3D) cell cul-

tures [22]. Compared with control vector transfected MCF10A (10A.vec) cells, ErbB2-overexpression in 10A.B2 cells led to a dramatic increase of p110 α and p-Akt-S473 levels, whereas knocking down of PIK3CA in 10A.B2 cells clearly reduced the levels of p110 α and p-Akt-S473 in both 2D and 3D cell cultures (**Figure 1C**). Knocking down PIK3CA in 10A.B2 cells significantly inhibited cell growth compared with 10A.B2 shctrl cells in 2D culture (*P* < 0.001; **Figure 1D**). In 3D cell culture, the 10A.vec cells formed smooth and polarized (laminin 5) spherical acinar structures with a hollow lumen that mimicked normal mammary glands *in vivo* (**Figure 1E**, first column from left), while 10A.B2 cells grew into large disorganized acinar structures with a filled lumen due to reduced apoptosis (cleaved caspase 3) and increased proliferation (Ki-67; **Figure 1E**, second column from left). Knocking down PIK3CA in 10A.B2 cells restored the spherical acini structure with a hollow lumen, similar to that of the 10A.vec cells (**Figure 1E**, first and second column from right). Immunofluorescent staining of the acini showed insignificant increases in apoptosis (cleaved caspase-3) with PIK3CA knockdown despite restoration of hollow lumens, whereas proliferation (Ki-67) was markedly reduced in PIK3CA-knockdown 10A.B2 cells (**Figure 1E**). Our further analyses indicated that knocking down PIK3CA not only significantly reduced the percentage of transformed acini but also decreased acini sizes (**Figure 1F, 1G**).

Next, we tested whether GDC-0941, a PI3K/Akt inhibitor that has been tested in clinical trials, can reverse transformed phenotype of 10A.B2 MECs in a manner similar to genetic knockdown of PIK3CA. Indeed, GDC-0941 treatment significantly reduced P-Akt-S473 in 10A.B2 cells in a concentration-dependent manner under both 2D and 3D cell culture conditions (**Figure 2A**). In addition, GDC-0941 significantly inhibited 10A.B2 cell growth (*P* < 0.001) but had only a marginal effect on 10A.vec cells (**Figure 2B**). Low-dose (0.3 μ M) GDC-0941 didn't significantly increase total apoptotic (early and late apoptosis) 10A.B2 cells, while high-dose (3 μ M) GDC-0941 significantly enhanced apoptosis of 10A.B2 cells (**Figure S2A**). Both low-dose and high-dose GDC-0941 induced apoptosis in N202 cells, a mammary tumor cell line derived from MMTV-*neu* mice

PI3K inhibitor enhances immune surveillance in breast cancer

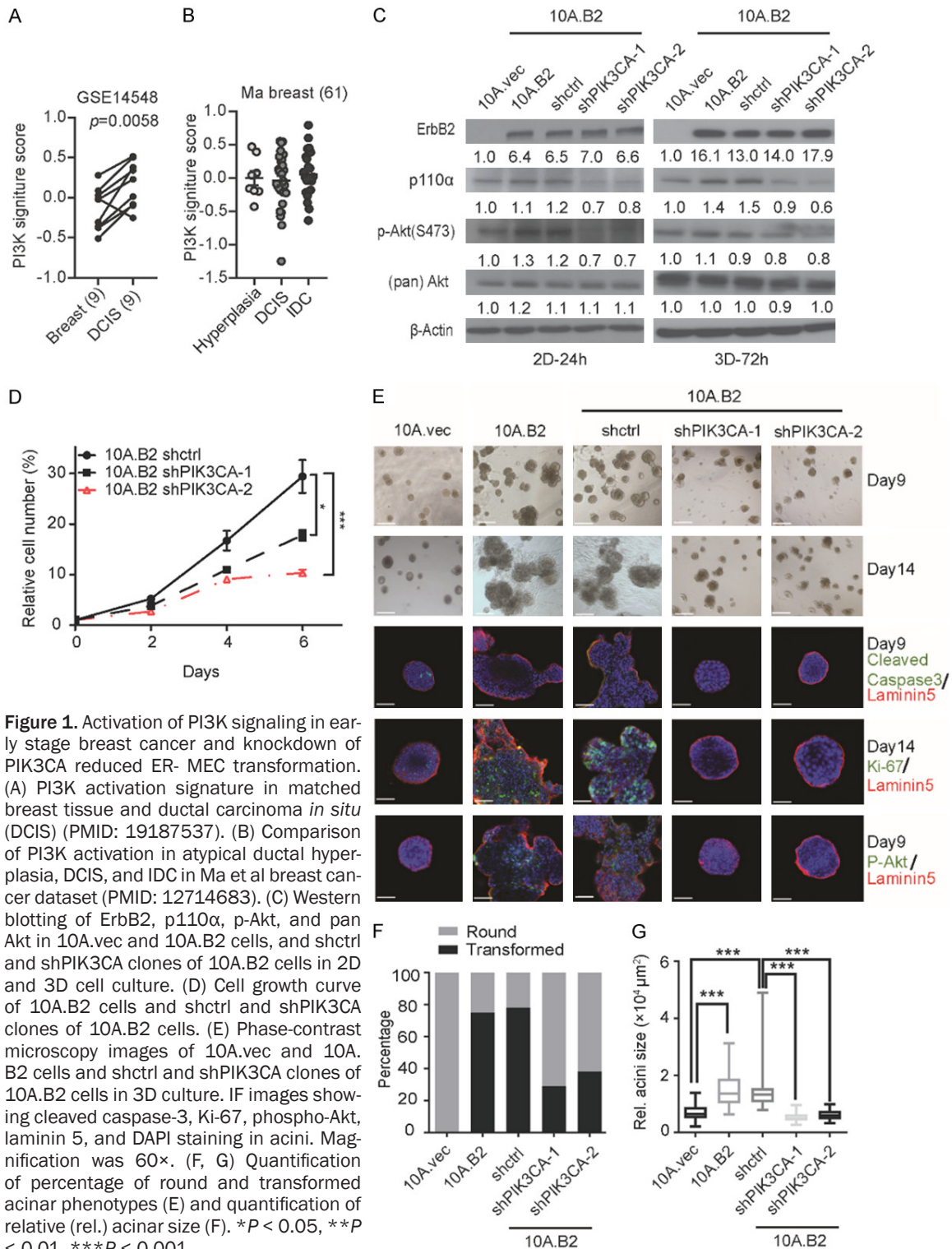


Figure 1. Activation of PI3K signaling in early stage breast cancer and knockdown of PIK3CA reduced ER- MEC transformation. (A) PI3K activation signature in matched breast tissue and ductal carcinoma *in situ* (DCIS) (PMID: 19187537). (B) Comparison of PI3K activation in atypical ductal hyperplasia, DCIS, and IDC in Ma et al breast cancer dataset (PMID: 12714683). (C) Western blotting of ErbB2, p110 α , p-Akt, and pan Akt in 10A.vec and 10A.B2 cells, and shctrl and shPIK3CA clones of 10A.B2 cells in 2D and 3D cell culture. (D) Cell growth curve of 10A.B2 cells and shctrl and shPIK3CA clones of 10A.B2 cells. (E) Phase-contrast microscopy images of 10A.vec and 10A.B2 cells and shctrl and shPIK3CA clones of 10A.B2 cells in 3D culture. IF images showing cleaved caspase-3, Ki-67, phospho-Akt, laminin 5, and DAPI staining in acini. Magnification was 60 \times . (F, G) Quantification of percentage of round and transformed acinar phenotypes (E) and quantification of relative (rel.) acinar size (F). * $P < 0.05$, ** $P < 0.01$, *** $P < 0.001$.

[20] (Figure S2B). In 3D cell culture, low-dose (0.3 μM) GDC-0941 significantly reversed the disorganized “grape-like” acini phenotype of 10A.B2 cells back to spherical acini similar to the 10A.vec cells, with reduced Ki67-positive

proliferating cells but insignificant change of apoptosis (Figure 2C). GDC-0941 treatment also significantly reduced the sizes of the 10A.B2 acinar compared with acini treated with vehicle (Figure 2D, 2E).

PI3K inhibitor enhances immune surveillance in breast cancer

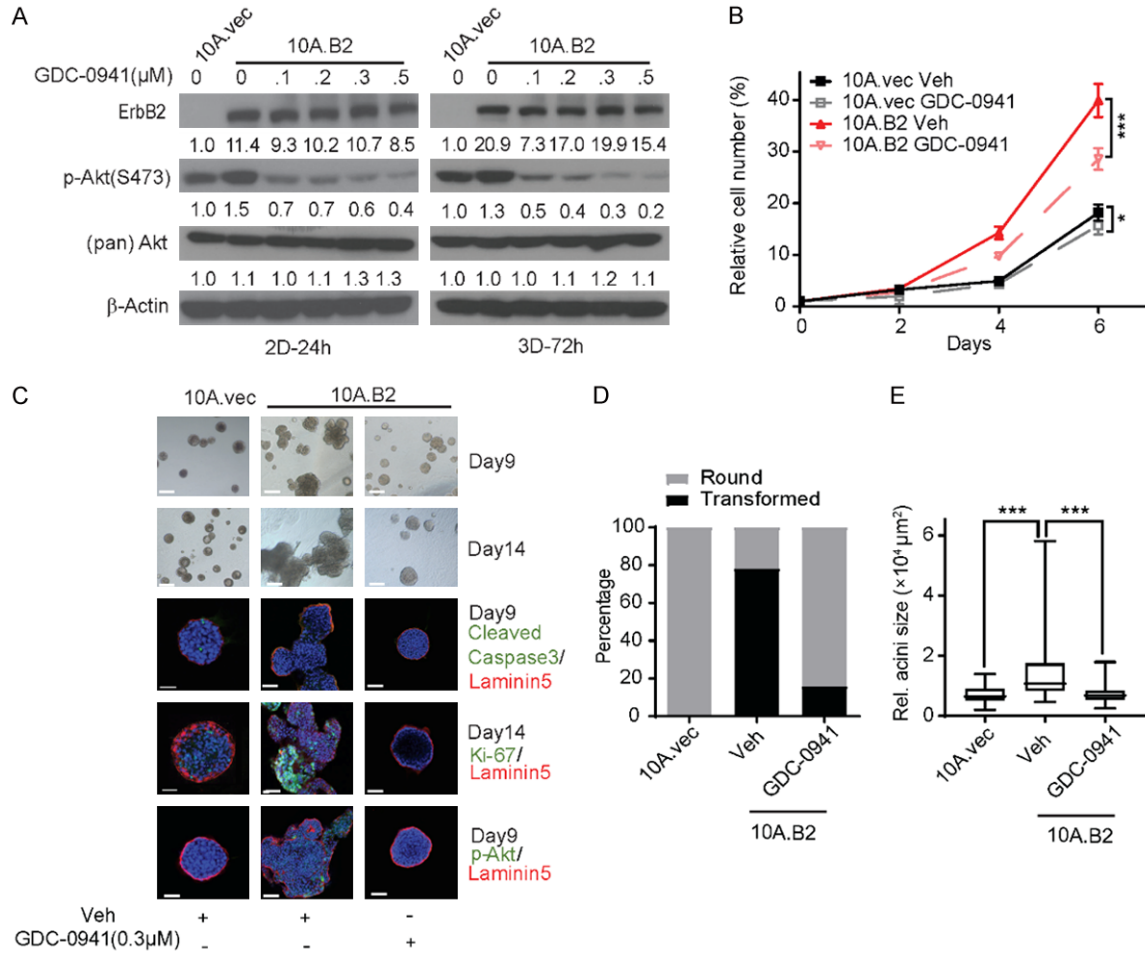


Figure 2. PI3K inhibitor GDC-0941 prevents disorganized acini formation of early ER- MECs. (A) Western blotting of ErbB2, p-Akt, and pan Akt in 10A.vec and 10A.B2 cells treated with GDC-0941 at various doses. (B) Cell growth curve of 10A.vec and 10A.B2 cells treated with GDC-0941. DMSO was used as vehicle control. (C) Microscopy images of 10A.vec and 10A.B2 cells grown in 3D culture for 9 days and 14 days, treated with DMSO or GDC-0941. Immunofluorescent images showing Ki-67 (on day 14), cleaved caspase-3 (on day 9), p-Akt, laminin 5, and DAPI staining in 10A.vec and 10A.B2 acini treated with vehicle or GDC-0941. Magnification was 60×. (D, E) Quantification of percentage of round and transformed acinar phenotypes (D) and quantification of relative (rel.) acinar size (E).

Together, these data indicated that PI3K/Akt activation is critical in early transformation of 10A.B2 MECs, and blocking PI3K/Akt activation by PIK3CA knockdown or low dose inhibitor rescues, at least partially, the dysplasia phenotype.

Targeting PI3K/Akt by GDC-0941 prolonged tumor-free survival of MMTV-*neu* mice

Encouraged by the *in vitro* data above, we further tested whether GDC-0941 administration would inhibit mammary tumor initiation in the wild-type *neu* (*neu* is the rat homologue of the human *ERBB2/HER2* gene) transgenic mouse model of MMTV-*neu* 202 Mul/J (denoted as

MMTV-*neu*) [29]. MMTV-*neu* mice develop ER-mammary intraepithelial neoplasia (MIN) at about 10 to 18 weeks and invasive ductal carcinoma (IDC) lesions at approximately 30 weeks, respectively [2]. The well-tolerated GDC-0941 dose in clinic is 330 mg/day, equivalent to 75-150 mg/kg/day in mice [30]. Our dose toxicity evaluations, including body weight, hematology and blood chemistry analyses, showed that GDC-0941 was well tolerated at the dosages of 20 and 100 mg/kg/day with no discernable toxicity (Figure 3A, 3B; Table S1). For potential clinical prevention application, we need to apply a lower dose GDC-0941 that minimize potential side effects while preserving most of its biological activities. We treated

PI3K inhibitor enhances immune surveillance in breast cancer

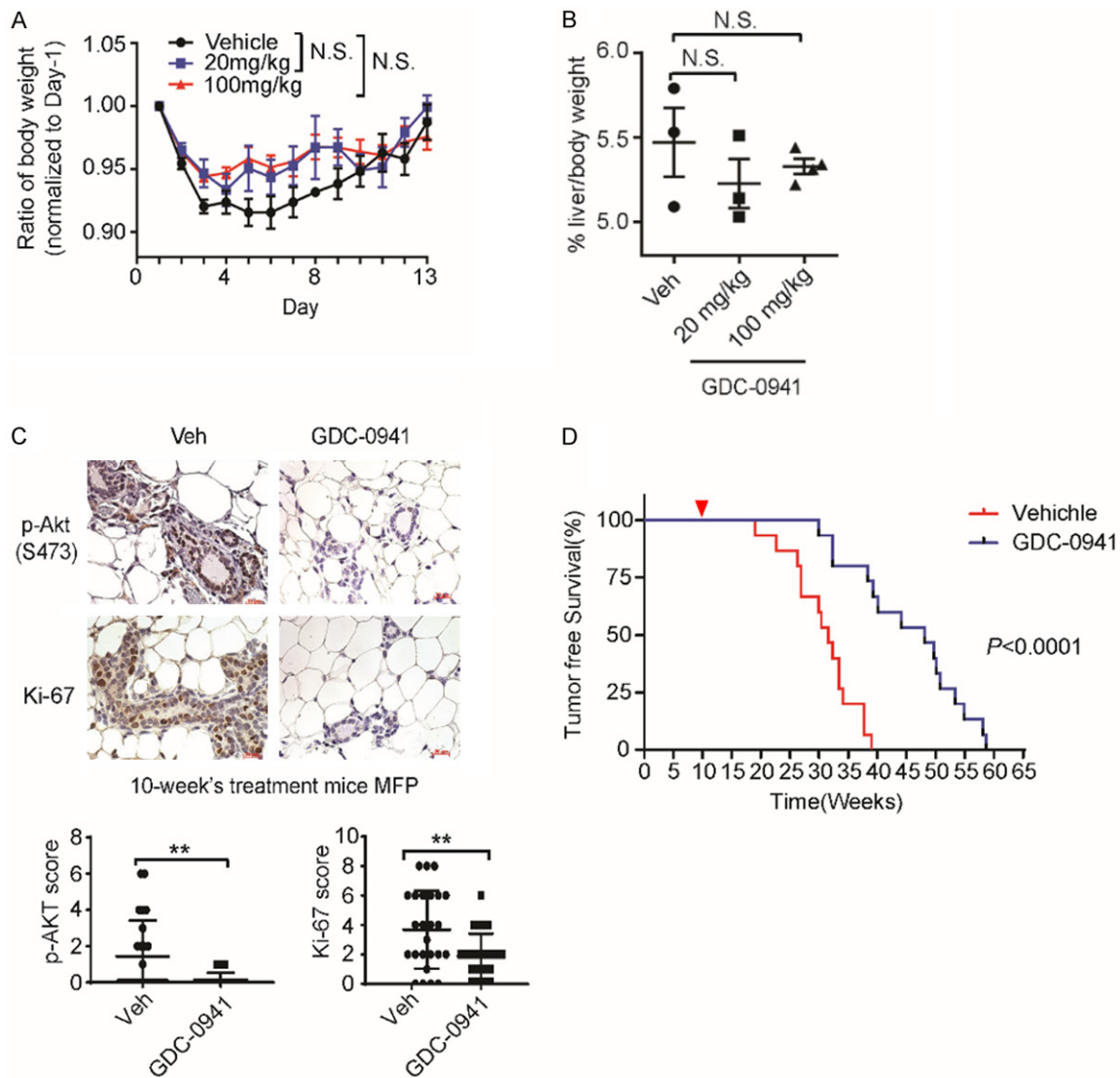


Figure 3. PI3K inhibitor GDC-0941 prolongs tumor-free survival in MMTV-*neu* mouse model. A. Ratio of total body weight in FVB mice treated with oral gavage of vehicle (n=3) or GDC-0941 at 20 mg/kg (n=3) and 100 mg/kg (n=4) for 2 weeks. B. Percentage of liver/body weight in FVB mice treated with oral gavage of vehicle (n=3) or GDC-0941 at 20 mg/kg (n=3) and 100 mg/kg (n=4) for 2 weeks. C. Representative images and quantification from immunohistochemistry staining for p-Akt and Ki-67 in MFPs of 10-week's vehicle- or GDC-0941-treated MMTV-*neu* mice. The respective scores are shown at the bottom. Magnification was 40 \times . D. Kaplan-Meier tumor-free survival curve in MMTV-*neu* mice treated with either vehicle (n=15, red) or GDC-0941 (n=15, blue) starting at week 10 (pointed by red triangle). Treatment was stopped when palpable tumor was detected in mouse.

MMTV-*neu* mice (n=29 per group) with 50 mg/kg/day low dose GDC-0941 starting at 10 weeks of age. 50 mg/kg/day GDC-0941 didn't show significant impact on the body weight of treated mice compared with that of vehicle treated mice after 6-week's treatment (Figure S3A), suggesting that the dose was well tolerated. Mammary fat pads (MFPs) from multiple vehicle- and GDC-0941-treated mice were collected after 10-week's treatment, and immunohistochemical (IHC) staining was performed to

examine the impacts of GDC-0941 treatment on PI3K pathway activation, mammary epithelial cell proliferation, and apoptosis. The levels of p-Akt-S473 and Ki-67 in mammary epithelial cells from the GDC-0941-treated group were significantly reduced compared with that of the vehicle-treated group (Figure 3C), indicating that low-dose GDC-0941 effectively inhibited PI3K pathway and mammary epithelial cell proliferation *in vivo*. On the other hand, no significant differences of apoptotic cells were detect-

ed in the MFPs between the two groups ([Figure S3B](#)). To examine whether low dose GDC-0941 treatment would delay mammary tumor initiation, mice in the vehicle- and GDC-0941-treated groups were evaluated for tumor-free survival. Briefly, mouse was treated with vehicle or GDC-0941 starting at week 10, and the treatment continued until palpable tumor was detected in mouse. By the week of 39, all the mice in the vehicle group (n=15) developed mammary tumors, while 11 out of the 15 mice in the GDC-0941-treated group remained tumor-free ([Figure 3D](#)). Indeed, low dose GDC-0941 treatment significantly extended the median tumor-free survival of the mice from 31.6 weeks (vehicle group) to 48.1 weeks (GDC-0941 group) ([Figure 3D](#)). Altogether, these data demonstrated that targeting PI3K/Akt with low dose GDC-0941 delayed tumor initiation and increased tumor-free survival in MMTV-*neu* mouse model of ER- mammary tumors.

*Low-dose GDC-0941 increases T-cell infiltration in mammary tissues of MMTV-*neu* mice*

PTEN loss and PI3K/Akt activation in tumor cells are associated with immune evasion, reduced T-cell infiltration, and resistance to immunotherapy in certain types of cancer [18, 31]. Thus, we explored whether GDC-0941 delayed mammary tumor initiation in MMTV-*neu* mice not only by inhibiting mammary epithelial cell proliferation ([Figure 3C](#)) but also by influencing T-cell infiltration in the TME. We examined immune cell infiltration in MFPs of 10-week's-veh-or GDC-0941-treated mice by immunofluorescent staining. Indeed, compared with vehicle treated mice, low-dose GDC-0941 treatment significantly increased CD3⁺ total T-lymphocytes and CD8⁺ T lymphocytes ([Figure 4A, 4B](#)) in MFPs compared with that of vehicle-treated mice. Additionally, immunohistochemistry also showed increased infiltration of GZMB⁺ cytotoxic T cells in MFPs from GDC-0941 treated mice compared to vehicle control mice ([Figure 4C](#)), suggesting enhanced immune surveillance by low dose GDC-0941 treatment. To test whether GDC-0941 would affect T-cells directly, low (0.3 μM) and high (3 μM) doses of GDC-0941 were applied to spleen T-lymphocytes in the absence or presence of the N202 mammary tumor cells. Interestingly, in the absence of tumor cells, low-dose GDC-0941 slightly increased the percentage of CD8⁺ T-cells and enhanced T-cell activation (IFNγ⁺) as

well, while high-dose GDC-0941 significantly reduced CD8⁺ T-cell activation ([Figure S4](#)). On the other hand, under co-culture with the N202 mammary tumor cells derived from MMTV-*neu* mice [20], GDC-0941 did not significantly impact on the percentage and activation of CD8⁺ T-cells ([Figure 4D, 4E](#)), suggesting that other mechanisms, such as enhanced T-cell recruitment, may contribute to increased T-cell infiltration in GDC-0941-treated MFPs.

GDC-0941 enhances T-cell migration towards tumor cells

PTEN loss and PI3K/Akt activation could result in dysregulation of cytokines and chemokines, which may suppress T-cell migration [18]. To examine whether GDC-0941 modulates T-cell recruitment to tumor cells, N202 mammary tumor cells were treated with low-dose GDC-0941 (0.3 μM) or vehicle, overlaid into the plate well of the trans-well unit and co-cultured with splenocytes loaded in culture inserts of the trans-well plate. The migrated T-cells were then analyzed by flow cytometry ([Figure 5A](#)). CD3⁺ T-cells migrated toward N202 tumor cells but not to culture medium; migration of total CD3⁺ T-cells toward tumor cells was significantly increased by GDC-0941 treatment compared to vehicle treatment ([Figure 5B](#)). Tumor cells' recruitment of CD45⁺CD3⁻ immune cells, including B cells and myeloid cells, are similar between two treatments ([Figure 5C](#)). Furthermore, we detected significantly increased migrations of CD4⁺, CD8⁺, and IFN-γ⁺ CD8⁺ T-cells in response to low-dose GDC-0941 treatment of N202 tumor cells ([Figure 5D-F](#)). Importantly, GDC-0941 didn't significantly impact on T-cell migration in the absence of N202 tumor cells ([Figure 5B-F](#)), which suggested that low dose GDC-0941 modulate tumor cell-dependent chemotaxis migration of T-cells, but not random migration of T-cells. Next, we tested whether GDC-0941 also increases human lymphocytes migration towards human ER- breast cancer cells by seeding the HER2+ER- HCC-1569 human breast cancer cells in the plate well and human peripheral blood mononuclear cells (PBMCs) in culture inserts of the trans-well plate for migration assay. Indeed, significantly increased migration of human CD3⁺, CD4⁺, CD8⁺, and IFN-γ⁺ CD8⁺ T-cells were detected in trans-wells seeded with GDC-0941-treated HCC-1569 cells ([Figure 5G-J](#)), while migration of CD3⁻ immune cells

PI3K inhibitor enhances immune surveillance in breast cancer

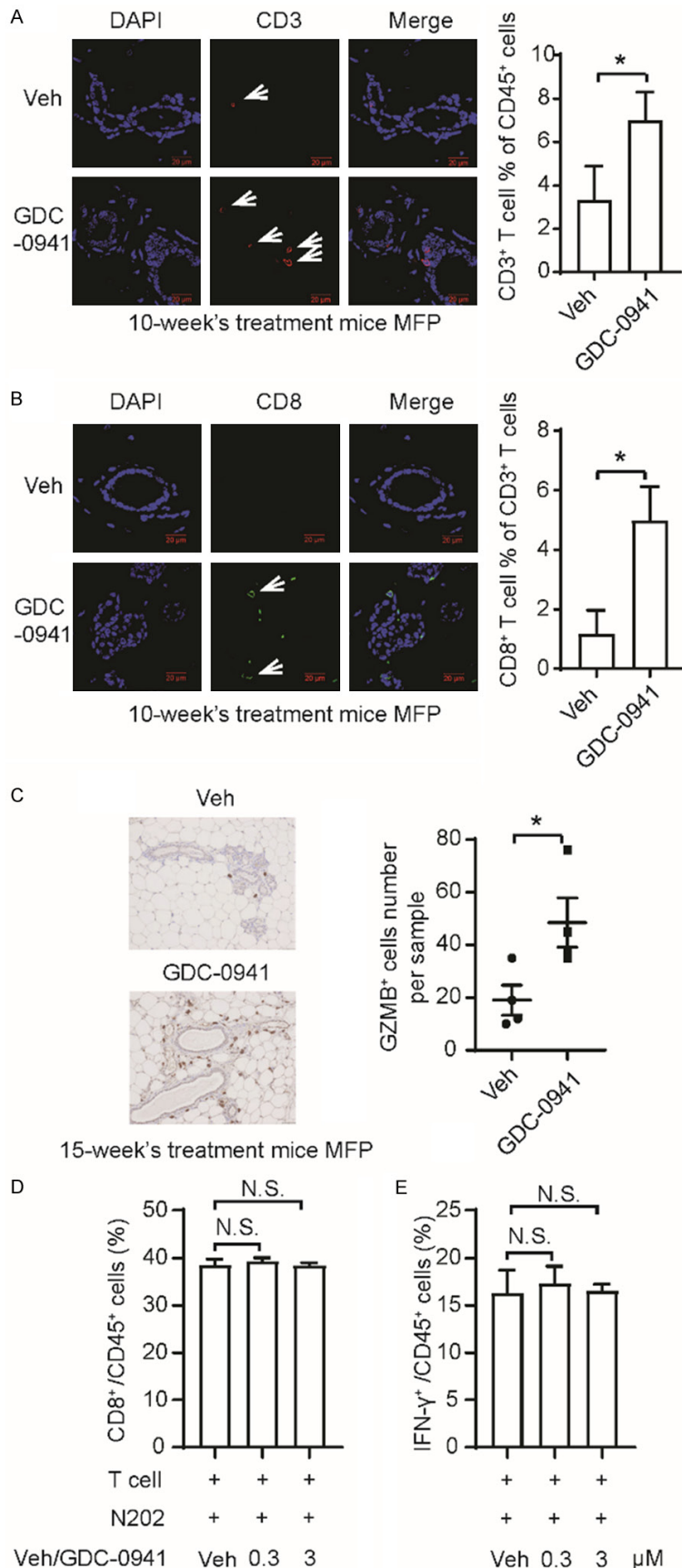


Figure 4. Low dose GDC-0941 treatment increased T-cell infiltration in MFPs of MMTV-*neu* mice. (A, B) Immunofluorescent staining and quantification of CD3⁺ T cells (A) and CD8⁺ T cells (B) in MFPs of 10-week's vehicle- and GDC-0941-treated MMTV-*neu* mice. The arrows pointed to CD3⁺ T cells and CD8⁺ T, respectively. Magnification was 60×. (C) Immunohistochemical staining and quantification of GZMB⁺ cells in MFPs of 15-week's vehicle- or GDC-0941-treated MMTV-*neu* mice. Magnification was 20×. (D) Percentage of CD8⁺/CD45⁺ cells of splenocytes after co-culture with 0.3 μM vs 3 μM GDC-0941-pretreated N202 cells. (E) IFN-γ⁺ percentage in CD45⁺ cells of splenocytes after co-culture with 0.3 μM vs 3 μM GDC-0941-pretreated N202 cells. **P* < 0.05, ***P* < 0.01, ****P* < 0.001.

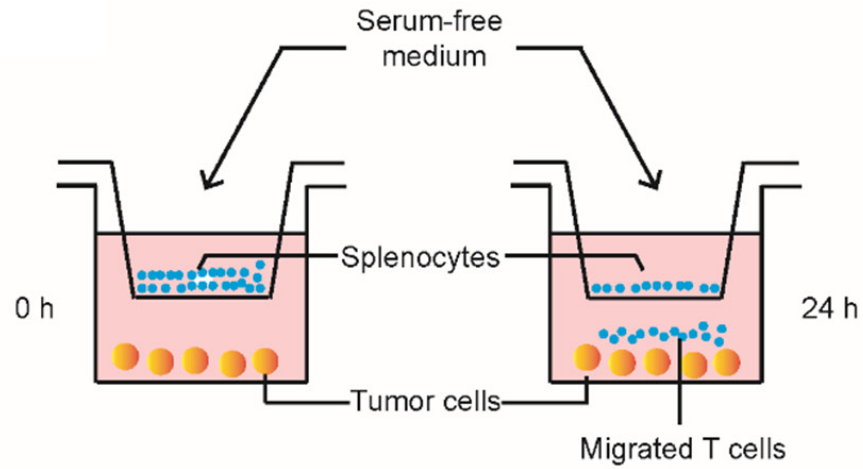
didn't change significantly (Figure 5K). Conversely, reduced migration of human CD3⁺, CD4⁺, CD8⁺ T lymphocytes and IFN-γ⁺ CD8⁺ T-cells were detected in PI3K pathway activated 10A.B2 cells compared with that of 10A.vec cells (Figure S5A-D). Altogether, our data indicate that PI3K pathway activation in mouse and human ER- breast cancer cells may contribute to T-cell suppression and inhibiting PI3K activation in tumor cells by low dose GDC-0941 enhances T-cell chemotaxis migration.

GDC-0941 enhances T-cell migration via CCL5/CXCL10

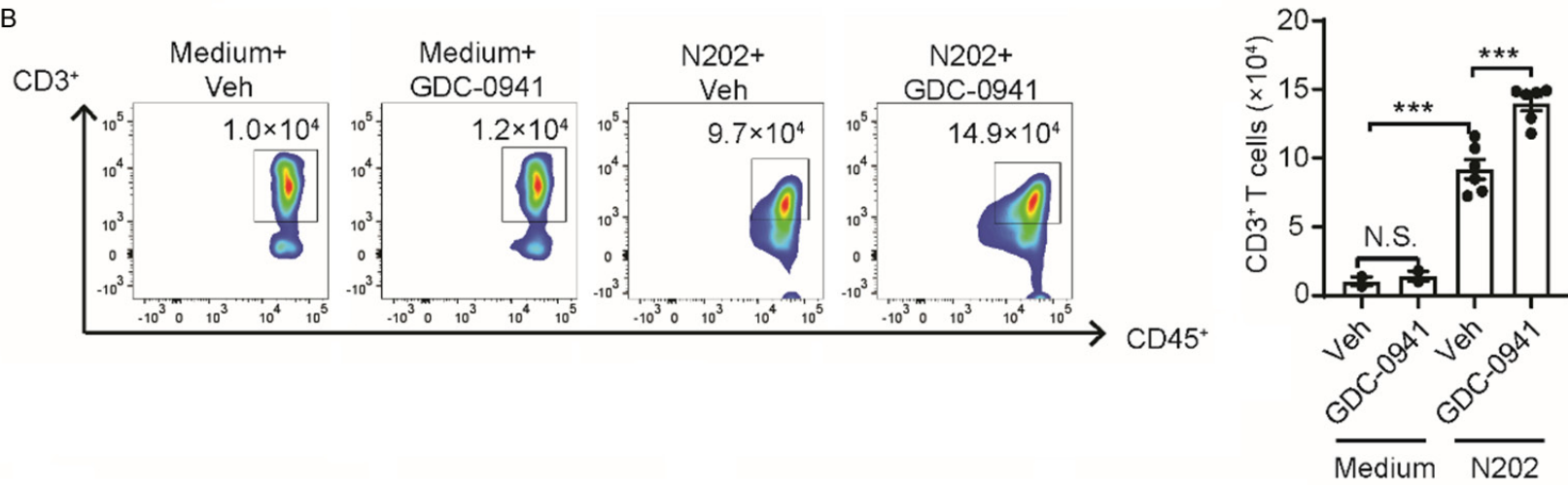
Next, we investigated how inhibition of PI3K/Akt in tumor cells by low dose GDC-0941 enhances T-cell chemotaxis. We examined mRNA expression levels of well-known T-cell-attracting chemokines, such as CCL5, CXCL9, and CXCL10, in response to GDC-0941 treatment in ER- murine mammary tumor cells, such as

PI3K inhibitor enhances immune surveillance in breast cancer

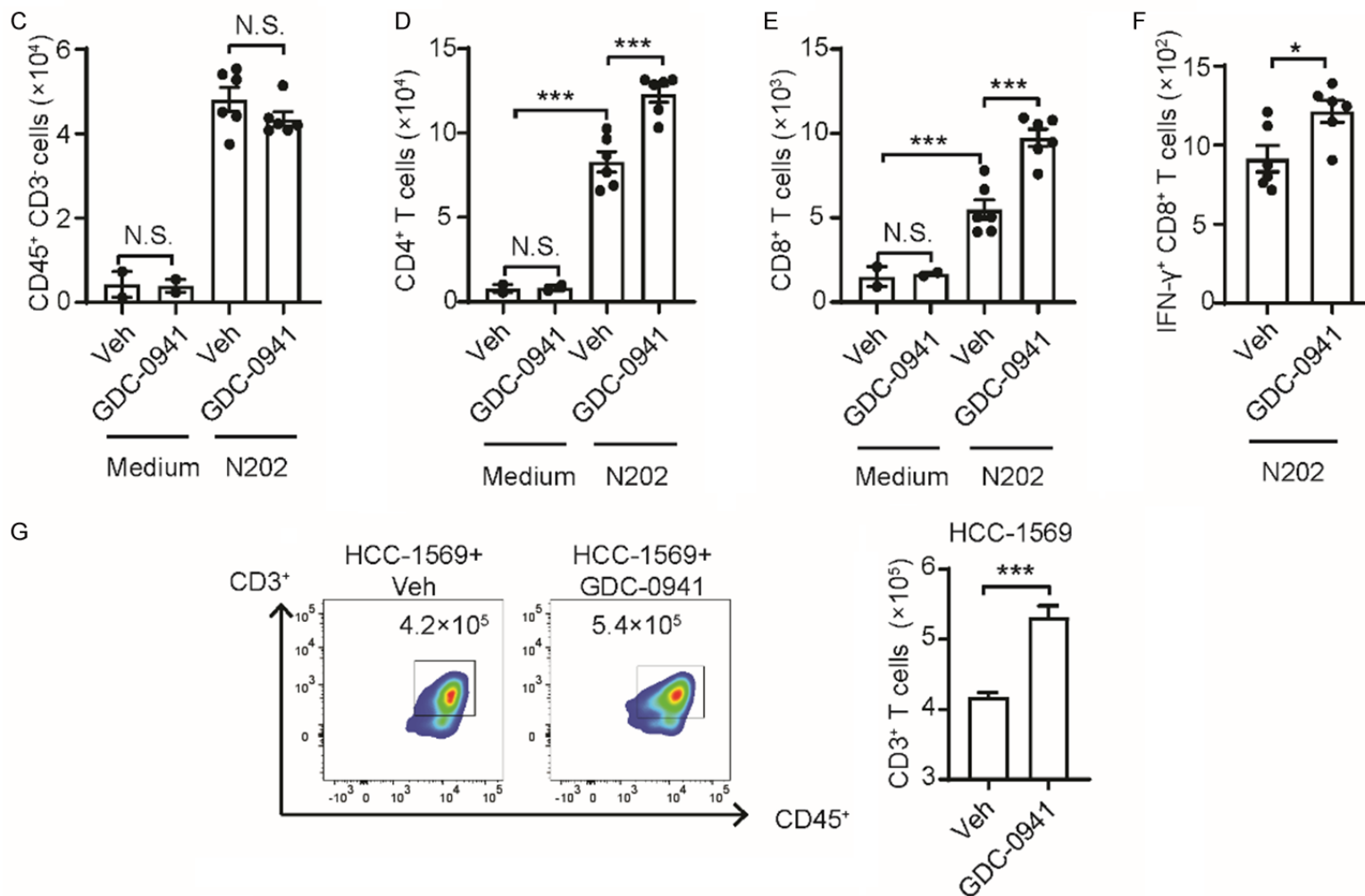
A



B



PI3K inhibitor enhances immune surveillance in breast cancer



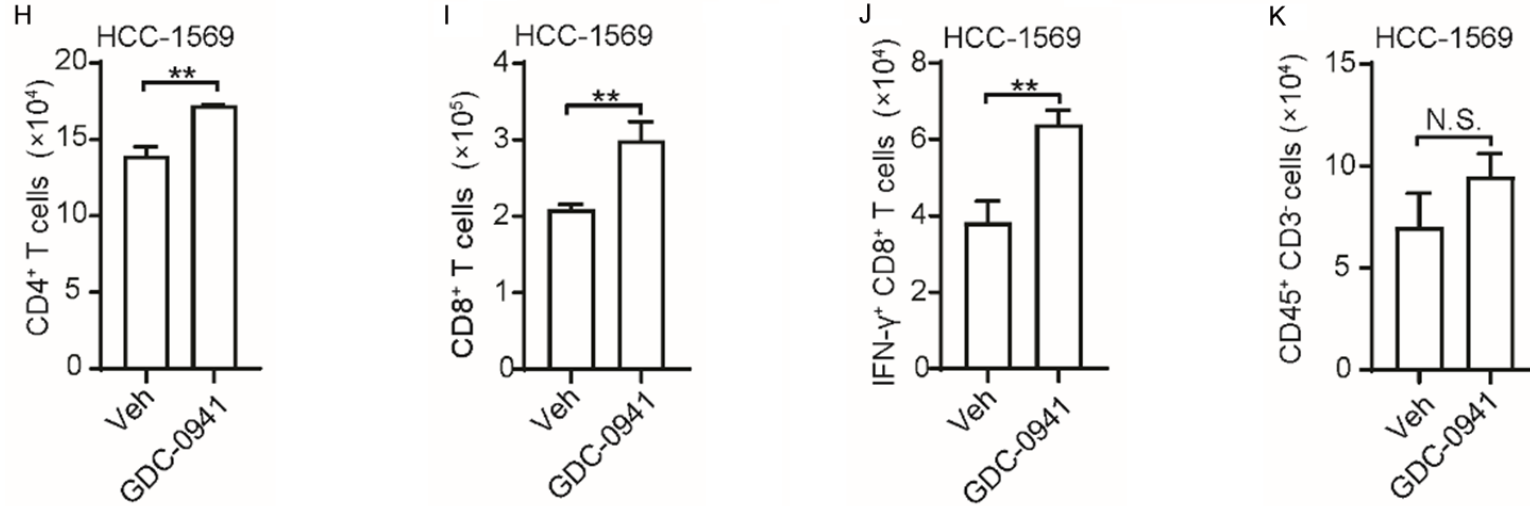


Figure 5. Low dose GDC-0941 enhances tumor cell-dependent T-cell recruitment. A. *In vitro* model of T-cell recruitment. B. Representative figures and quantification of mouse CD3⁺ T cells migrating to vehicle- and 0.3 μM GDC-0941-treated medium or N202 cells. C-F. Quantification of mouse CD45⁺CD3⁻, CD4⁺, CD8⁺ and IFN-γ⁺ CD8⁺ cells migrating to vehicle- and 0.3 μM GDC-0941-treated N202 cells. G. Representative figures and quantification of human CD3⁺ T cells migrating to vehicle- and 0.3 μM GDC-0941-treated HCC-1569 cells. H-K. Quantification of human CD4⁺, CD8⁺, IFN-γ⁺ CD8⁺, and CD45⁺CD3⁻ cells migrating to vehicle- and 0.3 μM GDC-0941-treated HCC-1569 cells. Each experiment had performed 3-6 times. **P* < 0.05, ***P* < 0.01, ****P* < 0.001.

PI3K inhibitor enhances immune surveillance in breast cancer

N202 and McNeuA generated from MMTV-*neu* transgenic mice, as well as human breast cancer cells. RT-PCR analysis detected increased mRNA levels of *ccl5* and *cxcl10* in murine mammary tumor cells (N202 and McNeuA) and human breast cancer cell HCC-1569 after inhibition of PI3K/Akt by GDC-0941 (0.3 μ M) treatment *in vitro* (Figures 6A, S6A, 6B, S7A). Consistently, GDC-0941 treatment *in vivo* also increased *ccl5* and *cxcl10* mRNA expressions in MFPs of MMTV-*neu* mice compared with those of vehicle-treated mice (Figure 6B). Both *in vitro* and *in vivo* data suggest that GDC-0941 treatment can upregulate T-cell-attracting chemokines *ccl5* and *cxcl10* expressions in mammary tumor cells.

To test whether CCL5 and CXCL10 mediate GDC-0941 treatment-induced T-cell chemotactic migration towards mammary tumor cells, CCL5 and CXCL10 blocking antibodies were applied individually or in combination to GDC-0941-pretreated N202 cells under co-cultured with T-cells. Indeed, blockade of either CCL5 or CXCL10 alone significantly inhibited GDC-0941 treatment-induced CD3⁺, CD4⁺, CD8⁺, and IFN γ ⁺ CD8⁺ T-cell migrations to N202 tumor cells (Figure 6C-F). Combination of anti-CCL5 and anti-CXCL10 antibodies inhibited T-cell migration with a slightly better trend (Figure 6C-F). Similarly, anti-human CCL5 blocking antibody also inhibited human CD3⁺, CD4⁺, CD8⁺, and IFN γ ⁺ CD8⁺ T-cell migration to GDC-0941-treated HCC-1569 cells (Figure S7B-E). However, CXCL10 antibody did not show much effect on human T-cell migration (Figure S7B-E). We found that the HCC-1569 cells without GDC-0941 treatment already express CXCL10 at a very high level (data not shown), it is possible that the CXCL10 antibody can't sufficiently block CXCL10 or/and CXCL10 is not a major mediator of GDC-0941-induced human PBMC T-cell migration. To further test the role of CXCL10 in human T-cell recruitment, we knocked down CXCL10 in HCC-1569 cells by siRNAs (Figure S8A). Knocking down of CXCL10 in HCC-1569 cells indeed abolished enhanced human T-cell migration in response to GDC-0941 treatment with minimal effects on migration of other immune cells in human PBMC (Figure S8B-F). Taken together, these data indicate that PI3K/Akt inhibition in mammary tumor cells upregulates critical T-cell-attracting chemokines, including CCL5 and CXCL10, which mediate T-cell chemotactic migration.

PI3K activation in human ER- breast cancer is associated with reduced CD8A, CCL5 and CXCL10

Above data suggest that PI3K activation suppresses CCL5 and CXCL10 expressions resulting in decreased T-cell recruitment and the escape of immune surveillance. To examine the relevance of our finding in human ER- breast cancer patients, we examined whether PI3K activation signature may correlate with CCL5, CXCL10, and CD8A expressions in human ER- breast cancer using dataset from the Cancer Genome Atlas (TCGA). Indeed, elevated PI3K activation based on a 32-gene expression signature [25], is associated with significantly reduced expressions of CD8A, CCL5, and CXCL10 (Figure 7A). Moreover, CD8A expression shows strong positive correlations with CCL5 and CXCL10 expressions, consistent with their critical roles in T-cell recruitment (Figure 7B). We further validated these findings in another ER- breast cancer patient cohort (GSE20685) which yielded similar results, although PI3K activation signature only showed a trend of negative association with CXCL10 expression which exhibited a relatively weak correlation with CD8A expression (Figure 7C, 7D). Altogether, these data support that PI3K activation is associated with significantly reduced expression of T-cell-attracting chemokines and CD8⁺ T-cell infiltration, which could contribute to immune evasion in ER- breast cancer (Figure 8).

Discussion

Dysregulation of the PI3K/Akt/mTOR/p70S6K pathway has been found in multiple types of cancer, including breast cancer, and it confers proliferation advantages that promote malignant transformation and tumorigenesis [32-34]. Our bioinformatics analysis in precancerous patient samples revealed that PI3K/Akt activation occurred at very early stage (e.g., hyperplasia) of ER- breast cancer development, suggesting that targeting the PI3K/Akt pathway might prevent hyperplasia transition to early tumor initiation. A growing number of kinase inhibitors have shown remarkable clinical efficacy in cancer treatment and been approved by the US Food and Drug Administration [35]. However, kinase inhibitors have not been keenly considered for cancer prevention due to toxic effects associated with the high doses used for treatment of late stage cancer. Here, we pro-

PI3K inhibitor enhances immune surveillance in breast cancer

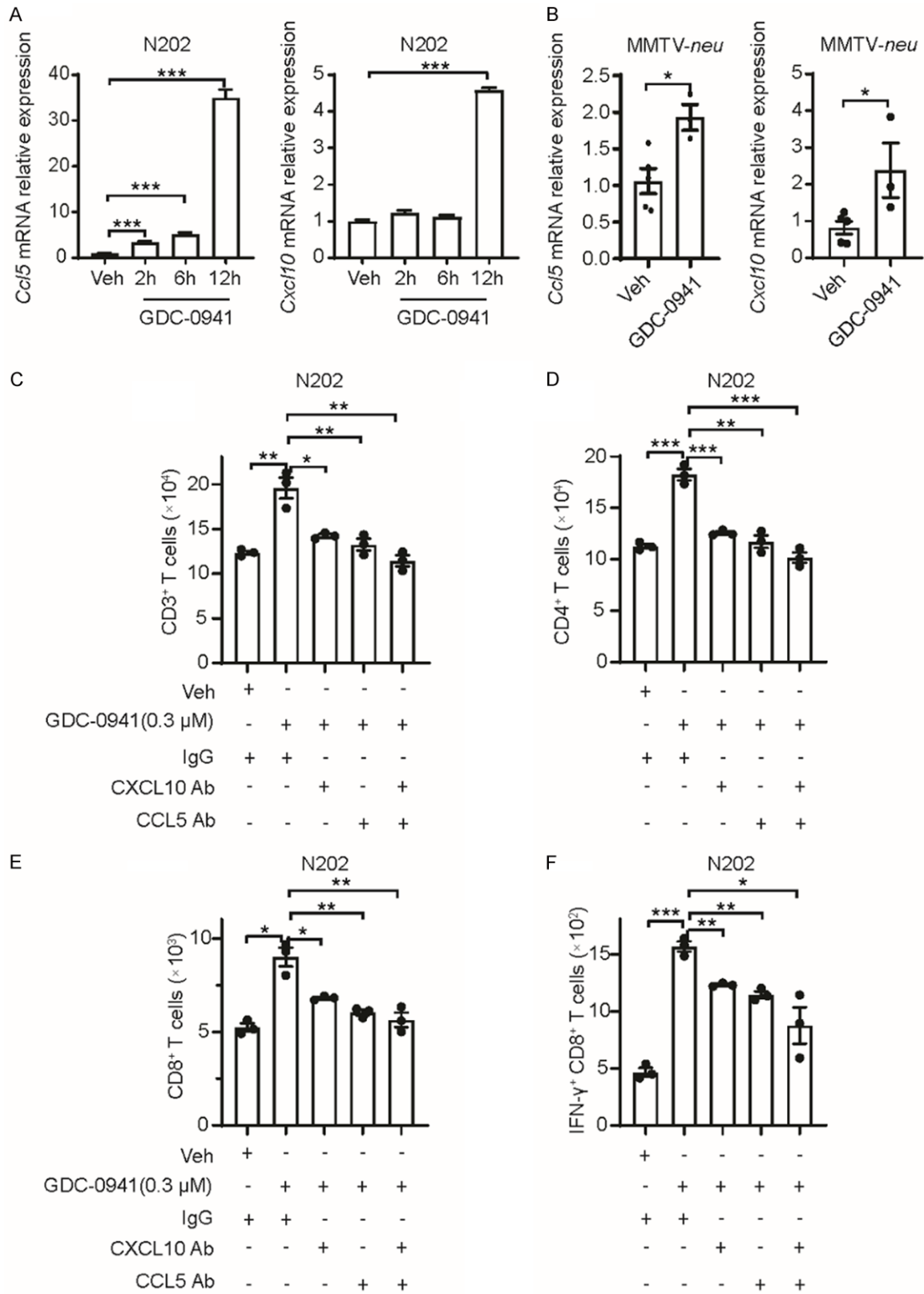


Figure 6. Low dose GDC-0941 increases CCL5/CXCL10 expression in tumor cells and enhances CCL5/CXCL10 dependent T-cell chemotaxis migration. A. mRNA expression of *ccl5* and *cxcl10* after vehicle and 2 h, 6 h, and 12 h of 0.3 μ M GDC-0941 treatment in N202 cells. B. mRNA expression of *ccl5* and *cxcl10* after vehicle and GDC-0941 treatment in MFP in 20-week-old MMTV-*neu* mice. C-F. Quantification of mouse CD3⁺, CD4⁺, CD8⁺ and IFN- γ ⁺ CD8⁺ cells under IgG control or anti-CCL5 antibody or anti-CXCL10 antibody treatment followed by GDC-0941 in N202 cells. Each experiment had performed 3 times. * $P < 0.05$, ** $P < 0.01$, *** $P < 0.001$.

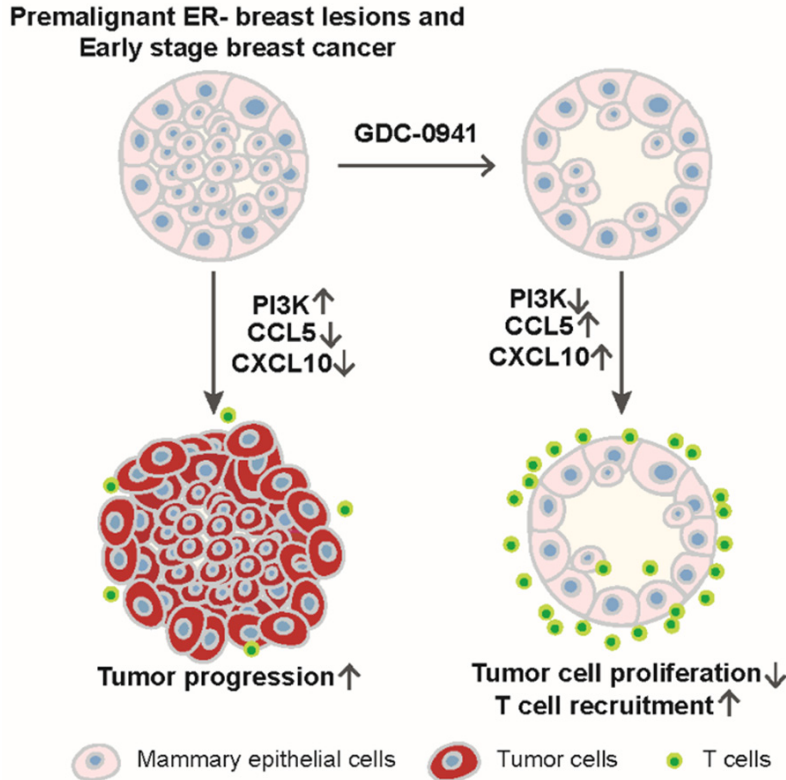


Figure 8. Schematic showing that PI3K/Akt is elevated in early stage of ER-breast cancer and inhibiting the PI3K/Akt pathway with low-dose GDC-0941 effectively inhibited ER- mammary tumor initiation by both inhibiting MEC proliferation and by increasing T-cell recruitment in a CCL5/CXCL10-dependent manner to enhance immune surveillance.

pose a novel approach of using highly specific, low-dose kinase inhibitors with low toxicity to target PI3K/Akt for preventing early-lesion transition to early-stage breast cancer. In a phase 2 clinical trial, GDC-0941 was tested and suppressed tumor cell proliferation [36]. Our data showed that PI3K/Akt inhibition by genetic knockdown or low dose GDC-0941 both significantly reduced disorganized acinar growth of the semi-transformed 10A.B2 human mammary epithelial cells in 3D cell culture (Figures 1E-G, 2C-E). More importantly, low-dose treatment with GDC-0941 in MMTV-*neu* mice was effective in suppressing Akt phosphorylation, decreasing cell proliferation, delaying mammary tumor initiation, and prolonging tumor-free survival (Figure 3C, 3D) without inducing apparent adverse effects (Figure 3A, 3B; Table S1).

In addition to their well-known roles in promoting cancer cell proliferation and resistance to apoptosis, PTEN loss and PI3K/Akt activation also help tumor cells to evade immune surveillance during tumor evolution. Here, we found

that inhibiting PI3K/Akt activation using low-dose GDC-0941 enhanced T-cell infiltration in mammary tissues surrounding DCIS-like lesions of MMTV-*neu* mice (Figure 4A, 4B). Although high dose GDC-0941 may inhibit T-cell activity *in vitro* (Figure S4B), low dose GDC-0941 had no significant toxicity in T-cells *in vitro* and no discernable adverse effects in mice during 20 or more weeks of treatment (Figures 3A, 3B, S4; Table S1). On the other hand, low-dose GDC-0941 treatment facilitated tumor cell-mediated T-cell chemotaxis, which is critical for immune surveillance (Figure 5). These data suggest that enhanced immune surveillance in tumor microenvironment may also contribute to prolonged tumor-free survival in GDC-0941-treated mice on top of targeting tumor cells themselves.

Our screening of chemokines expressed by mammary tumor cells that are involved in GDC-0941-facilitated T-cell infiltration revealed that, two potent chemoattractant for T-cells, CCL5 and CXCL10, were significantly up-regulated after GDC-0941 treatment and contributed to T-cell chemotaxis migration in both mouse and human breast cancer cells (Figures 6A, S6A, 6B, S7A). On the other hand, chemokines involved in myeloid migration, such as CCL2, CXCL2, and CXCL5, did not show significant changes in response to PI3K/Akt inhibition in tumor cells (data not shown), consistent with minimal alterations of CD45⁺CD3⁻ cell migration by GDC-0941 treatment *in vitro* (Figure 5C, 5K). A potential mediator of CCL5 and CXCL10 suppression by PI3K/Akt pathway is Erk5 since Erk5 knockout in prostate tissue of a Pten-deficient mouse model of prostate cancer significantly upregulated *cc15* and *cxcl10* expressions [19]. Additionally, the crucial roles of ERK5 overexpression in early stage breast cancer development [37] as well as breast cancer invasion/metastasis [38] have been suggest-

PI3K inhibitor enhances immune surveillance in breast cancer

ed. However, inhibiting PI3K pathway by GDC-0941 didn't affect p-Erk5 expression (data not shown), suggesting other downstream signals of PI3K pathway are involved in CCL5 and CXCL10 regulation, which warrants future investigation.

A limitation of our study is that only one PI3K inhibitor GDC-0941 was tested in our models. Very recently, two PI3K inhibitors predominantly targeting PI3K- α have been approved by FDA. One of them, alpelisib (BYL719), is approved for treatment of ER+ HER2- breast cancer in combination with endocrine therapy. It merits future testing to determine whether alpelisib has similar effects as that of GDC-0941 in prevention and early intervention of ER- breast cancer.

In summary, we identified PI3K/Akt activation as a potential target for ER- breast cancer prevention and showed that inhibiting the PI3K/Akt pathway by low-dose GDC-0941 effectively suppressed abnormal acini growth of semi-transformed mammary epithelial cells *in vitro* and delayed ER- mammary tumor initiation *in vivo*. In addition, low dose of PI3K inhibitor also significantly enhanced T-cell recruitment in a CCL5 and CXCL10-dependent manner (**Figure 8**). Cancer vaccines have shown efficacy in secondary prevention of HER2+ breast cancer [39]. It is anticipated that a low-dose PI3K inhibitor in combination with cancer vaccines may further improve the immunoprevention efficacy of cancer vaccines in breast cancer. Our data in this study, along with other novel findings [2, 14, 40], could serve as scientific bases of developing effective prevention strategies for ER- breast cancer in the future.

Acknowledgements

We thank Bryan Tutt of Scientific Publications of MD Anderson Cancer Center (MDACC) for manuscript editing. This work was supported by National Institutes of Health (NIH) grants R01-CA112567-06 (D.Y.), R01CA184836 (D.Y.), R01CA208213 (D.Y.), the METAVivor grants 56675 and 58284 (D.Y.), and NIH Cancer Center Support Grant P30CA016672 to MDACC (Functional Genomic Core, Flow Cytometry and Cellular Imaging Facility, Research Histology Core, Characterized Cell Line Core, and Research Animal Support Facility-Houston). We thank the Chinese Government Scholarship (J.W. NO.201608440317) for supporting

Jinyang Wang as a visiting PhD candidate in MDACC, and The Sixth Affiliated Hospital of Guangzhou Medical University for supporting Yuan Zhang as a Postdoc Fellow in MDACC. Dr. Yu is the Hubert L. & Olive Stringer Distinguished Chair in Basic Science, MDACC.

Disclosure of conflict of interest

None.

Address correspondence to: Dihua Yu and Yi Xiao, Department of Molecular and Cellular Oncology, The University of Texas MD Anderson Cancer Center, 6565 MD Anderson Blvd., Unit 108, Houston, Texas 77030-4009, USA. Tel: 713-792-3636; Fax: 713-792-4544; E-mail: dyu@mdanderson.org (DHY); yxiao2@mdanderson.org (YX)

References

- [1] Fisher B, Costantino JP, Wickerham DL, Cecchini RS, Cronin WM, Robidoux A, Bevers TB, Kavanah MT, Atkins JN, Margolese RG, Runowicz CD, James JM, Ford LG and Wolmark N. Tamoxifen for the prevention of breast cancer: current status of the National Surgical Adjuvant Breast and Bowel Project P-1 study. *J Natl Cancer Inst* 2005; 97: 1652-1662.
- [2] Jain S, Wang X, Chang CC, Ibarra-Drendall C, Wang H, Zhang Q, Brady SW, Li P, Zhao H, Dobbs J, Kyrish M, Tkaczyk TS, Ambrose A, Sistrunk C, Arun BK, Richards-Kortum R, Jia W, Seewaldt VL and Yu D. Src inhibition blocks c-Myc translation and glucose metabolism to prevent the development of breast cancer. *Cancer Res* 2015; 75: 4863-4875.
- [3] Jordan VC. Tamoxifen for breast cancer prevention. *Proc Soc Exp Biol Med* 1995; 208: 144-149.
- [4] Fisher B, Costantino JP, Wickerham DL, Redmond CK, Kavanah M, Cronin WM, Vogel V, Robidoux A, Dimitrov N, Atkins J, Daly M, Wieand S, Tan-Chiu E, Ford L and Wolmark N. Tamoxifen for prevention of breast cancer: report of the National Surgical Adjuvant Breast and Bowel Project P-1 Study. *J Natl Cancer Inst* 1998; 90: 1371-1388.
- [5] Vogel VG, Costantino JP, Wickerham DL, Cronin WM, Cecchini RS, Atkins JN, Bevers TB, Fehrenbacher L, Pajon ER Jr, Wade JL 3rd, Robidoux A, Margolese RG, James J, Lippman SM, Runowicz CD, Ganz PA, Reis SE, McCaskill-Stevens W, Ford LG, Jordan VC and Wolmark N; National Surgical Adjuvant Breast and Bowel Project (NSABP). Effects of tamoxifen vs raloxifene on the risk of developing invasive breast cancer and other disease outcomes: the

PI3K inhibitor enhances immune surveillance in breast cancer

- NSABP Study of Tamoxifen and Raloxifene (STAR) P-2 trial. *JAMA* 2006; 295: 2727-2741.
- [6] King D, Yeomanson D and Bryant HE. PI3K the lock: targeting the PI3K/Akt/mTOR pathway as a novel therapeutic strategy in neuroblastoma. *J Pediatr Hematol Oncol* 2015; 37: 245-251.
- [7] Ojeda L, Gao J, Hooten KG, Wang E, Thonhoff JR, Dunn TJ, Gao T and Wu P. Critical role of PI3K/Akt/GSK3beta in motoneuron specification from human neural stem cells in response to FGF2 and EGF. *PLoS One* 2011; 6: e23414.
- [8] Olsz J, Doleschall Z, Dunai Z, Pazsitka A and Csuka O. PI3K/AKT pathway activation and therapeutic consequences in breast cancer. *Magy Onkol* 2015; 59: 346-351.
- [9] Delaloge S and DeForceville L. Targeting PI3K/AKT pathway in triple-negative breast cancer. *Lancet Oncol* 2017; 18: 1293-1294.
- [10] Abraham J. PI3K/AKT/mTOR pathway inhibitors: the ideal combination partners for breast cancer therapies? *Expert Rev Anticancer Ther* 2015; 15: 51-68.
- [11] Kanaizumi H, Higashi C, Tanaka Y, Hamada M, Shinzaki W, Azumi T, Hashimoto Y, Inui H, Houchou T and Komoike Y. PI3K/Akt/mTOR signaling pathway activation in patients with ER-positive, metachronous, contralateral breast cancer treated with hormone therapy. *Oncol Lett* 2019; 17: 1962-1968.
- [12] Toska E, Osmanbeyoglu HU, Castel P, Chan C, Hendrickson RC, Elkabets M, Dickler MN, Scaltriti M, Leslie CS, Armstrong SA and Baselga J. PI3K pathway regulates ER-dependent transcription in breast cancer through the epigenetic regulator KMT2D. *Science* 2017; 355: 1324-1330.
- [13] Sanchez A and Villanueva J. PI3K-based molecular signatures link high PI3K pathway activity with low ER levels in ER+ breast cancer. *Expert Rev Proteomics* 2010; 7: 819-821.
- [14] Wang X, Yao J, Wang J, Zhang Q, Brady SW, Arun B, Seewaldt VL and Yu D. Targeting aberrant p70S6K activation for estrogen receptor-negative breast cancer prevention. *Cancer Prev Res (Phila)* 2017; 10: 641-650.
- [15] Sarker D, Ang JE, Baird R, Kristeleit R, Shah K, Moreno V, Clarke PA, Raynaud FI, Levy G, Ware JA, Mazina K, Lin R, Wu J, Fredrickson J, Spørke JM, Lackner MR, Yan Y, Friedman LS, Kaye SB, Derynck MK, Workman P and de Bono JS. First-in-human phase I study of pictilisib (GDC-0941), a potent pan-class I phosphatidylinositol-3-kinase (PI3K) inhibitor, in patients with advanced solid tumors. *Clin Cancer Res* 2015; 21: 77-86.
- [16] Nagarsheth N, Wicha MS and Zou W. Chemokines in the cancer microenvironment and their relevance in cancer immunotherapy. *Nat Rev Immunol* 2017; 17: 559-572.
- [17] Dangaj D, Bruand M, Grimm AJ, Ronet C, Barras D, Duttagupta PA, Lanitis E, Duraiswamy J, Tanyi JL, Benencia F, Conejo-Garcia J, Ramay HR, Montone KT, Powell DJ Jr, Gimotty PA, Facciabene A, Jackson DG, Weber JS, Rodig SJ, Hodi SF, Kandalaf LE, Irving M, Zhang L, Foukas P, Rusakiewicz S, Delorenzi M and Coukos G. Cooperation between constitutive and inducible chemokines enables T cell engraftment and immune attack in solid tumors. *Cancer Cell* 2019; 35: 885-900, e810.
- [18] Peng W, Chen JQ, Liu C, Malu S, Creasy C, Tetzlaff MT, Xu C, McKenzie JA, Zhang C, Liang X, Williams LJ, Deng W, Chen G, Mbofung R, Lazar AJ, Torres-Cabala CA, Cooper ZA, Chen PL, Tieu TN, Spranger S, Yu X, Bernatchez C, Forget MA, Haymaker C, Amaria R, McQuade JL, Glitza IC, Cascone T, Li HS, Kwong LN, Hefferman TP, Hu J, Bassett RL Jr, Bosenberg MW, Woodman SE, Overwijk WW, Lizee G, Roszik J, Gajewski TF, Wargo JA, Gershenwald JE, Radvanyi L, Davies MA and Hwu P. Loss of PTEN promotes resistance to T cell-mediated immunotherapy. *Cancer Discov* 2016; 6: 202-216.
- [19] Loveridge CJ, Mui EJ, Patel R, Tan EH, Ahmad I, Welsh M, Galbraith J, Hedley A, Nixon C, Blyth K, Sansom O and Leung HY. Increased T-cell infiltration elicited by Erk5 deletion in a pten-deficient mouse model of prostate carcinogenesis. *Cancer Res* 2017; 77: 3158-3168.
- [20] Campbell MJ, Wollish WS, Lobo M and Esserman LJ. Epithelial and fibroblast cell lines derived from a spontaneous mammary carcinoma in a MMTV/neu transgenic mouse. *In Vitro Cell Dev Biol Anim* 2002; 38: 326-333.
- [21] Xu J, Acharya S, Sahin O, Zhang Q, Saito Y, Yao J, Wang H, Li P, Zhang L, Lowery FJ, Kuo WL, Xiao Y, Ensor J, Sahin AA, Zhang XH, Hung MC, Zhang JD and Yu D. 14-3-3zeta turns TGF-beta's function from tumor suppressor to metastasis promoter in breast cancer by contextual changes of Smad partners from p53 to Gli2. *Cancer Cell* 2015; 27: 177-192.
- [22] Debnath J, Muthuswamy SK and Brugge JS. Morphogenesis and oncogenesis of MCF-10A mammary epithelial acini grown in three-dimensional basement membrane cultures. *Methods* 2003; 30: 256-268.
- [23] Lu J, Guo H, Treeritkarnmongkol W, Li P, Zhang J, Shi B, Ling C, Zhou X, Chen T, Chiao PJ, Feng X, Seewaldt VL, Muller WJ, Sahin A, Hung MC and Yu D. 14-3-3zeta cooperates with ErbB2 to promote ductal carcinoma in situ progression to invasive breast cancer by inducing epithelial-mesenchymal transition. *Cancer Cell* 2009; 16: 195-207.

PI3K inhibitor enhances immune surveillance in breast cancer

- [24] Campanella GS and Luster AD. Chapter 18. A chemokine-mediated in vivo T-cell recruitment assay. *Methods Enzymol* 2009; 461: 397-412.
- [25] Creighton CJ. A gene transcription signature of the Akt/mTOR pathway in clinical breast tumors. *Oncogene* 2007; 26: 4648-4655.
- [26] Ma XJ, Salunga R, Tuggle JT, Gaudet J, Enright E, McQuary P, Payette T, Pistone M, Stecker K, Zhang BM, Zhou YX, Varnholt H, Smith B, Gadd M, Chatfield E, Kessler J, Baer TM, Erlander MG and Sgroi DC. Gene expression profiles of human breast cancer progression. *Proc Natl Acad Sci U S A* 2003; 100: 5974-5979.
- [27] Kao KJ, Chang KM, Hsu HC and Huang AT. Correlation of microarray-based breast cancer molecular subtypes and clinical outcomes: implications for treatment optimization. *BMC Cancer* 2011; 11: 143.
- [28] Samuels Y, Wang Z, Bardelli A, Silliman N, Ptak J, Szabo S, Yan H, Gazdar A, Powell SM, Riggins GJ, Willson JK, Markowitz S, Kinzler KW, Vogelstein B and Velculescu VE. High frequency of mutations of the PIK3CA gene in human cancers. *Science* 2004; 304: 554.
- [29] Guy CT, Webster MA, Schaller M, Parsons TJ, Cardiff RD and Muller WJ. Expression of the neu protooncogene in the mammary epithelium of transgenic mice induces metastatic disease. *Proc Natl Acad Sci U S A* 1992; 89: 10578-10582.
- [30] Govindarajan B, Bai X, Cohen C, Zhong H, Kilroy S, Louis G, Moses M and Arbiser JL. Malignant transformation of melanocytes to melanoma by constitutive activation of mitogen-activated protein kinase kinase (MAPKK) signaling. *J Biol Chem* 2003; 278: 9790-9795.
- [31] Vidotto T, Melo CM, Castelli E, Koti M, Dos Reis RB and Squire JA. Emerging role of PTEN loss in evasion of the immune response to tumours. *Br J Cancer* 2020; 122: 1732-1743.
- [32] Yuan TL and Cantley LC. PI3K pathway alterations in cancer: variations on a theme. *Oncogene* 2008; 27: 5497-5510.
- [33] Luo J, Manning BD and Cantley LC. Targeting the PI3K-Akt pathway in human cancer: rationale and promise. *Cancer Cell* 2003; 4: 257-262.
- [34] Jiang BH and Liu LZ. PI3K/PTEN signaling in angiogenesis and tumorigenesis. *Adv Cancer Res* 2009; 102: 19-65.
- [35] Zhang J, Yang PL and Gray NS. Targeting cancer with small molecule kinase inhibitors. *Nat Rev Cancer* 2009; 9: 28-39.
- [36] Schmid P, Pinder SE, Wheatley D, Macaskill J, Zammit C, Hu J, Price R, Bundred N, Hadad S, Shia A, Sarker SJ, Lim L, Gazinska P, Woodman N, Korbie D, Trau M, Mainwaring P, Gendreau S, Lackner MR, Derynck M, Wilson TR, Butler H, Earl G, Parker P, Purushotham A and Thompson A. Phase II randomized preoperative window-of-opportunity study of the PI3K inhibitor pictilisib plus anastrozole compared with anastrozole alone in patients with estrogen receptor-positive breast cancer. *J Clin Oncol* 2016; 34: 1987-1994.
- [37] Montero JC, Ocana A, Abad M, Ortiz-Ruiz MJ, Pandiella A and Esparis-Ogando A. Expression of Erk5 in early stage breast cancer and association with disease free survival identifies this kinase as a potential therapeutic target. *PLoS One* 2009; 4: e5565.
- [38] Pavan S, Meyer-Schaller N, Diepenbruck M, Kalathur RKR, Saxena M and Christofori G. A kinome-wide high-content siRNA screen identifies MEK5-ERK5 signaling as critical for breast cancer cell EMT and metastasis. *Oncogene* 2018; 37: 4197-4213.
- [39] Crosby EJ, Gwin W, Blackwell K, Marcom PK, Chang S, Maecker HT, Broadwater G, Hyslop T, Kim S, Rogatko A, Lubkov V, Snyder JC, Osada T, Hobeika AC, Morse MA, Lysterly HK and Hartman ZC. Vaccine-induced memory CD8(+) T cells provide clinical benefit in HER2 expressing breast cancer: a mouse to human translational study. *Clin Cancer Res* 2019; 25: 2725-2736.
- [40] Li Y and Brown PH. Prevention of ER-negative breast cancer. *Recent Results Cancer Res* 2009; 181: 121-134.

PI3K inhibitor enhances immune surveillance in breast cancer

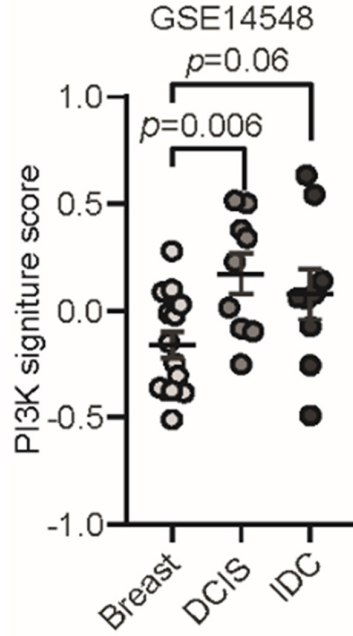
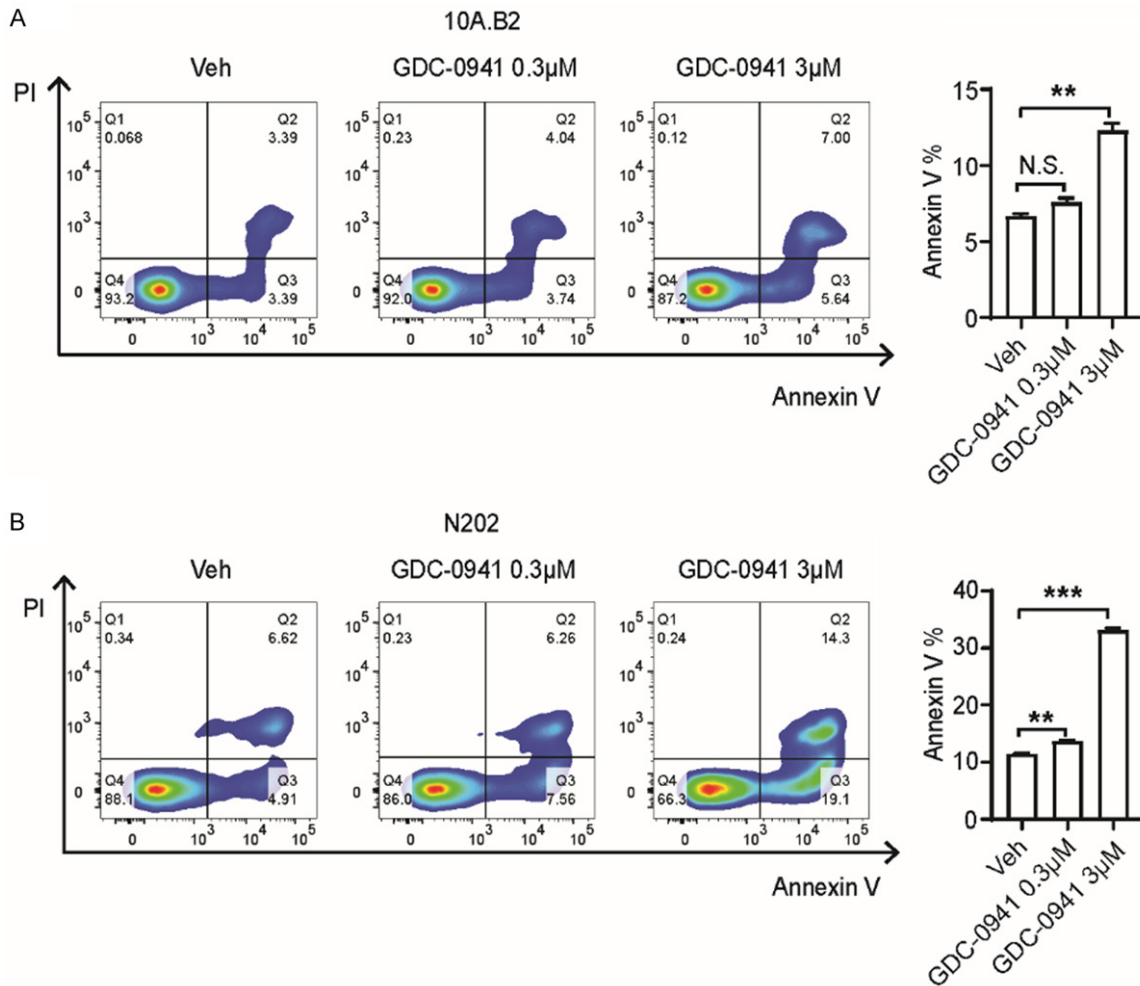


Figure S1. PI3K activation in different stages of early human breast cancer development. Comparison of PI3K activation between normal breast tissue vs DCIS vs Invasive ductal carcinoma (IDC) from GSE14548 dataset.



PI3K inhibitor enhances immune surveillance in breast cancer

Figure S2. Apoptosis upon low- vs high-dose GDC-0941 treatment in 10A.B2 and N202 cells. A. Flow cytometry results and quantitation of 0.3 μ M vs 3 μ M GDC-0941 treatment in 10A.B2 cells. B. Flow cytometry results and quantitation of 0.3 μ M vs 3 μ M GDC-0941 treatment in N202 cells. * $P < 0.05$, ** $P < 0.01$, *** $P < 0.001$.

Table S1. Toxicity of GDC-0941 in mice

	ALT (U/L)	AST (U/L)	CRE (mg/dL)	WBC ($\times 10^3/\mu$ L)	HG (g/dL)	PLT ($\times 10^3/\mu$ L)	Segs (%)	Lymphs (%)
Vehicle	51 \pm 22	226 \pm 144	0.28 \pm 0.03	3.41 \pm 1.77	14.2 \pm 0.5	810 \pm 32	12.0 \pm 9.0	79.2 \pm 8.1
GDC-0941 20 mg/kg	47 \pm 14	269 \pm 178	0.21 \pm 0.02	2.78 \pm 1.78	13.3 \pm 0.2	985 \pm 6	11.0 \pm 4.9	77.6 \pm 7.8
GDC-0941 100 mg/kg	51 \pm 3	181 \pm 103	0.25 \pm 0.04	1.73 \pm 0.09	14.0 \pm 0.0	952 \pm 242	12.0 \pm 0.0	78.5 \pm 2.1

Hematology and chemistry analyses in FVB mice treated with oral gavage of vehicle (n=3) or GDC-0941 at 20 mg/kg (n=3) and 100 mg/kg (n=4) for 2 weeks.

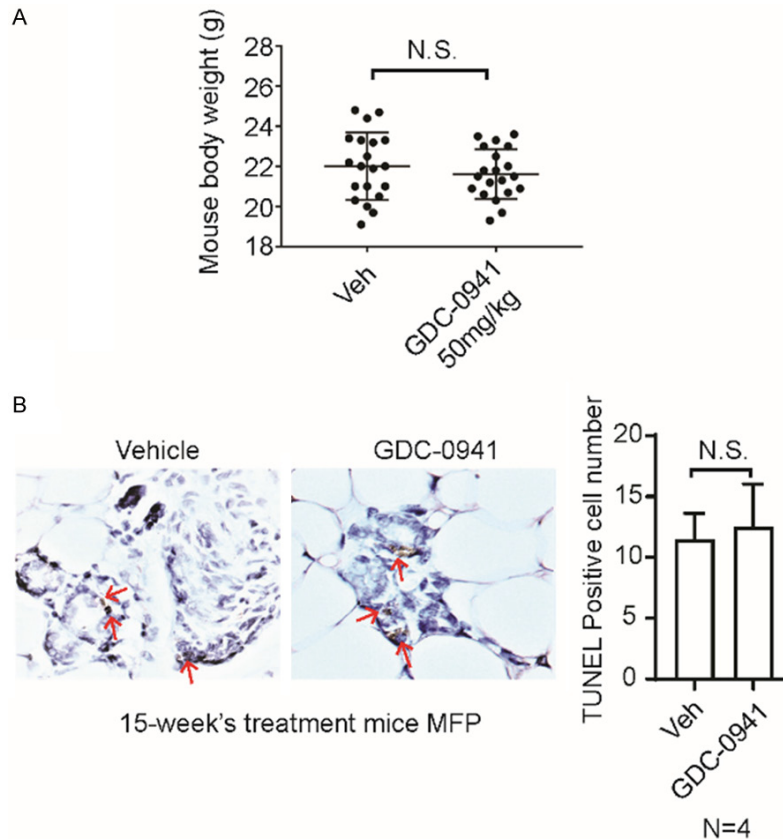


Figure S3. The impact of 50 mg/kg/day GDC-0941 treatment on mice. A. Body weight of mice after 6-week's treatment of vehicle or 50 mg/kg/day GDC-0941 (n=29 mice/per group). B. MEC apoptosis in GDC-0941-treated mice. Representative images and quantification from TUNEL assay in MFPs of 15-week's vehicle- or GDC-0941-treated MMTV-*neu* mice. Magnification was 40 \times . N=4 in each group. * $P < 0.05$, ** $P < 0.01$, *** $P < 0.001$.

PI3K inhibitor enhances immune surveillance in breast cancer

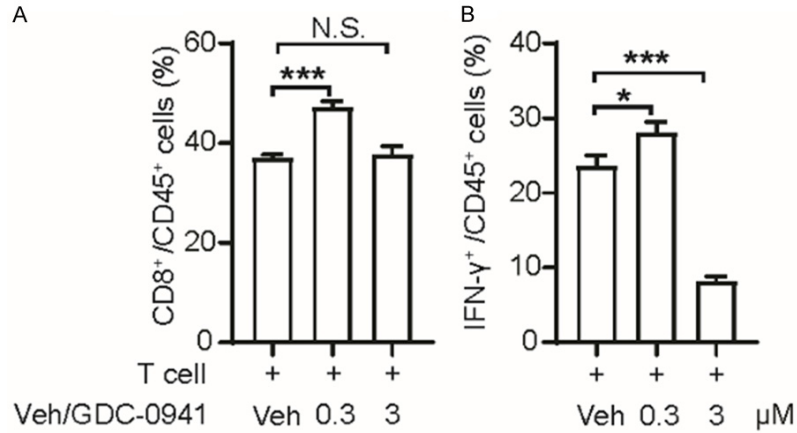


Figure S4. Effects of GDC-0941 on mouse CD8⁺ T cells. A. Percentage of CD8⁺/CD45⁺ cells of splenocytes after 0.3 μM vs 3 μM GDC-0941 treatment. B. IFN-γ⁺ percentage in CD45⁺ cells of splenocytes after 0.3 μM vs 3 μM GDC-0941 treatment. **P* < 0.05, ***P* < 0.01, ****P* < 0.001.

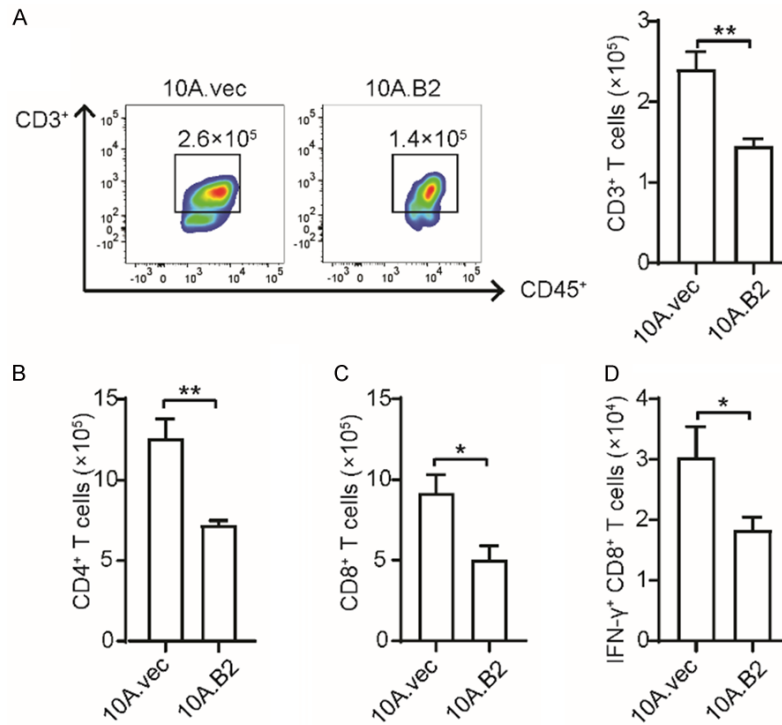


Figure S5. ErBb2 overexpression in human MECs inhibited human T-cell recruitment. A. Representative figures and quantification of human CD3⁺ T cells migrating to 10A.vec or 10A.B2 cells. B-D. Effects on human T-cell migration to 10A.vec and 10A.B2 cells. Quantification of human CD4⁺, CD8⁺ and IFN-γ⁺ CD8⁺ cells in vehicle- and 0.3 μM GDC-0941-treated 10A.vec and 10A.B2 cells. Each experiment had performed 3-6 times. **P* < 0.05, ***P* < 0.01, ****P* < 0.001.

PI3K inhibitor enhances immune surveillance in breast cancer

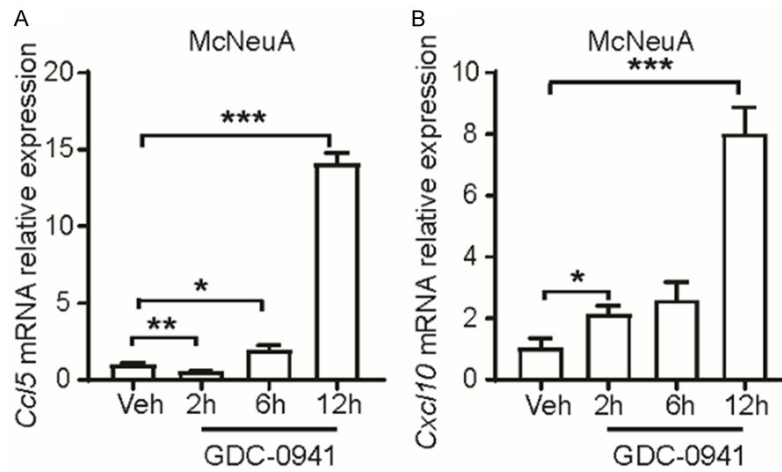


Figure S6. Effect of 0.3 μ M GDC-0941 on *cc15* and *cxcl10* mRNA in McNeuA cells. A. mRNA expression of *cc15* after vehicle and 2 h, 6 h, and 12 h of 0.3 μ M GDC-0941 treatment in McNeuA cells. B. mRNA expression of *cxcl10* after vehicle and 2 h, 6 h, and 12 h of 0.3 μ M GDC-0941 treatment in McNeuA cells. * P < 0.05, ** P < 0.01, *** P < 0.001.

PI3K inhibitor enhances immune surveillance in breast cancer

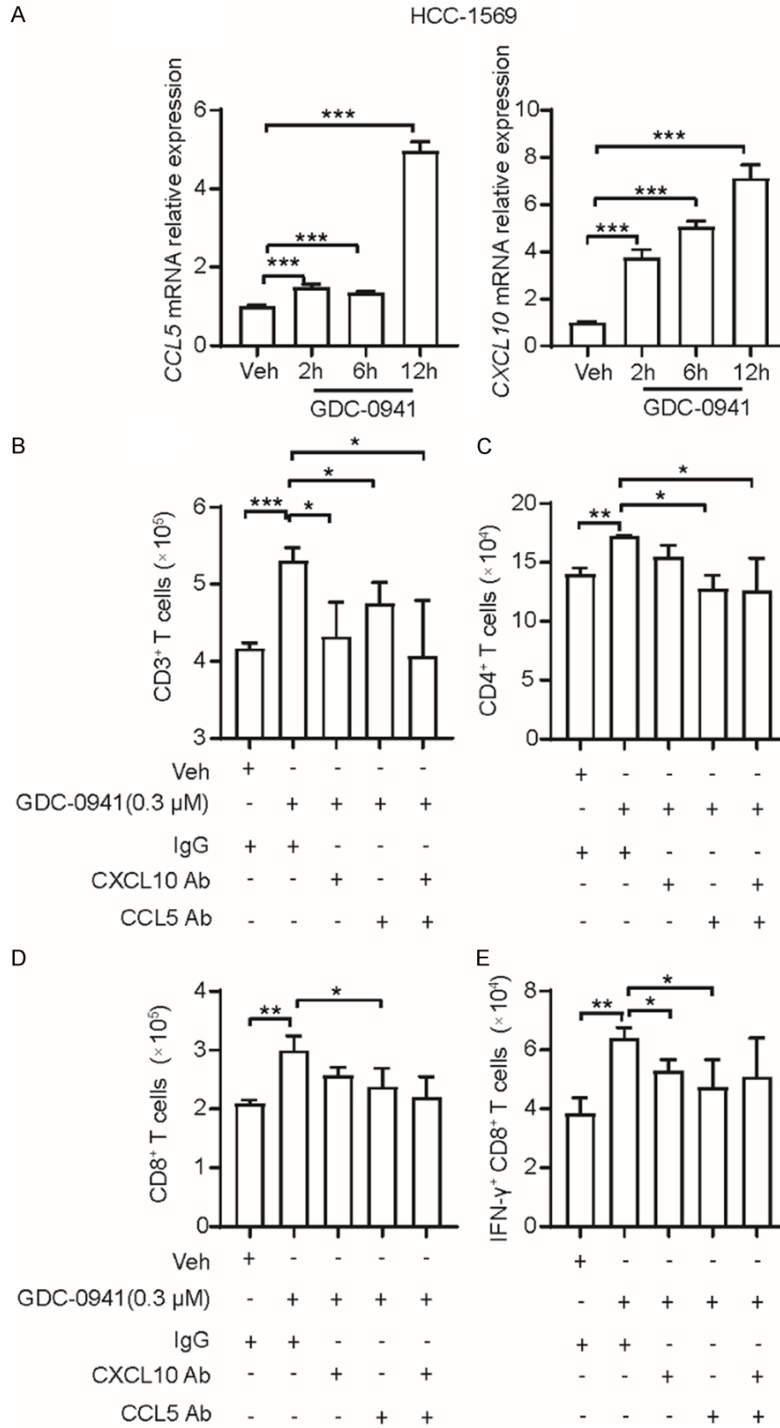


Figure S7. Low GDC-0941 treatment of HCC-1569 increases *CCL5*/*CXCL10* expression and enhances CCL5 dependent human T-cell recruitment. A. mRNA expression of *CCL5* and *CXCL10* after vehicle and 2 h, 6 h, and 12 h of 0.3 μM GDC-0941 treatment in HCC-1569 cells. B-E. Quantification of human CD3⁺, CD4⁺, CD8⁺ and IFN-γ⁺ CD8⁺ cells under IgG control or anti-CCL5 antibody or anti-CXCL10 antibody treatment followed by GDC-0941 in HCC-1569 cells. Each experiment had performed 3 times. **P* < 0.05, ***P* < 0.01, ****P* < 0.001.

PI3K inhibitor enhances immune surveillance in breast cancer

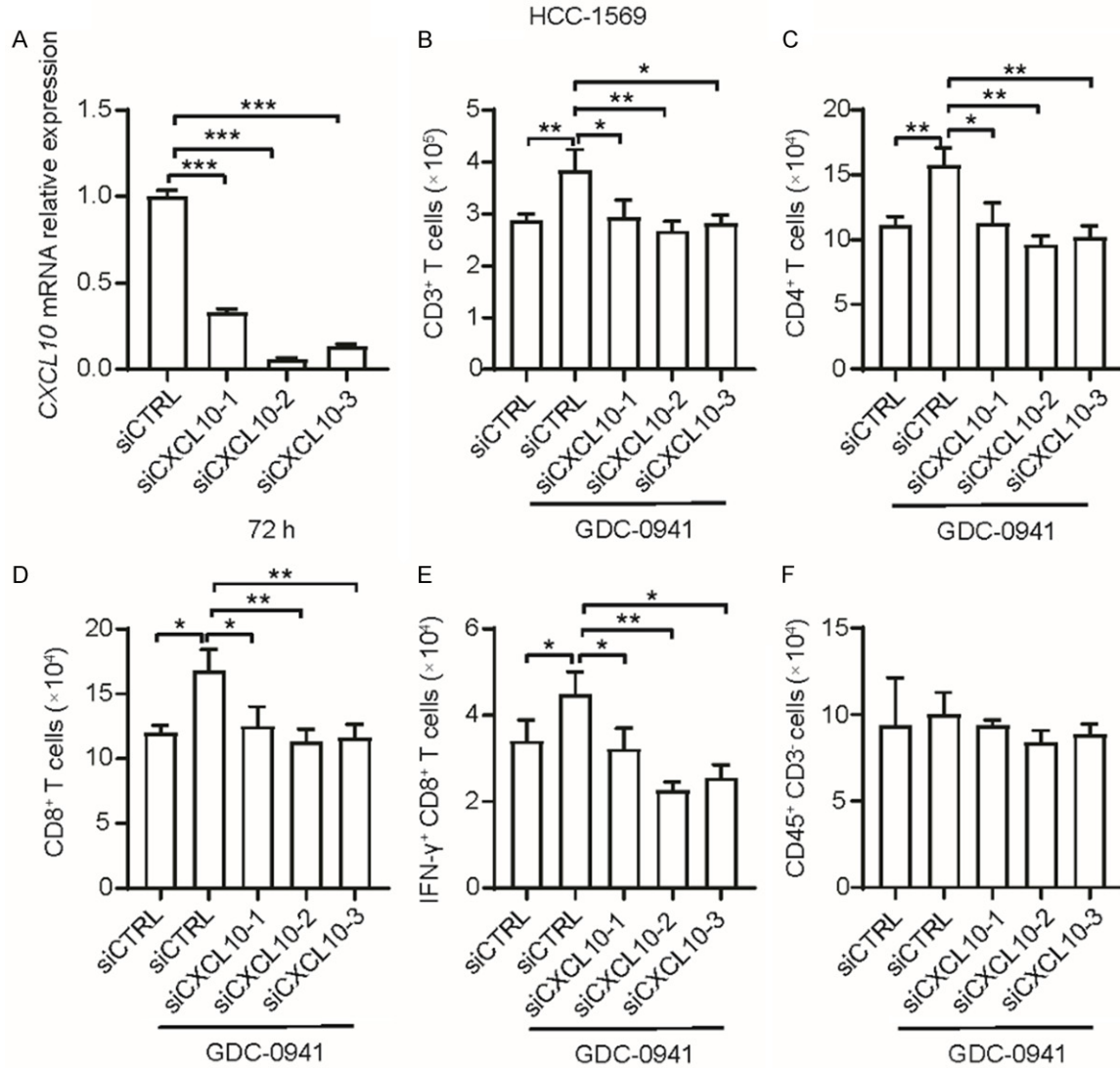


Figure S8. Knockdown CXCL10 in ER- HCC-1569 cells abolish low dose GDC-0941-mediated increased human T-cell recruitment. A. mRNA expression of CXCL10 after transfection of siCTRL, siCXCL10-1, siCXCL10-2 and siCXCL10-3 in HCC-1569 cells after 72 h. B-F. Quantification of human CD3⁺, CD4⁺, CD8⁺, IFN- γ ⁺ CD8⁺ and CD45⁺CD3⁺ cells migrating to HCC-1569 cells that were transfected with siCTRL or siCXCL10 and treated with GDC-0941. Each experiment had performed 3-4 times. * $P < 0.05$, ** $P < 0.01$, *** $P < 0.001$.